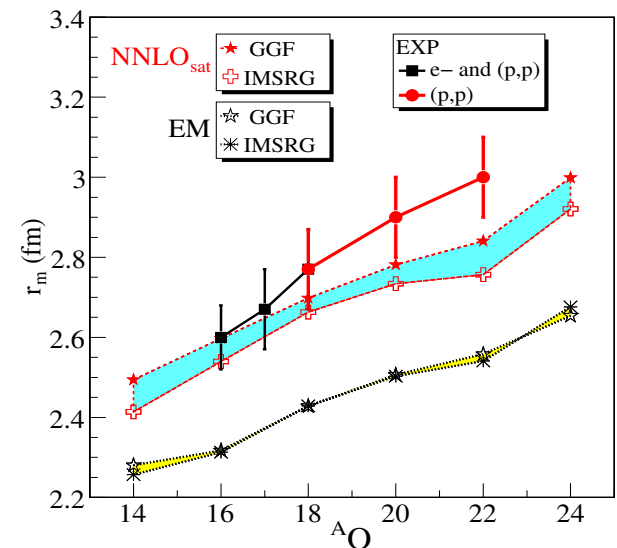
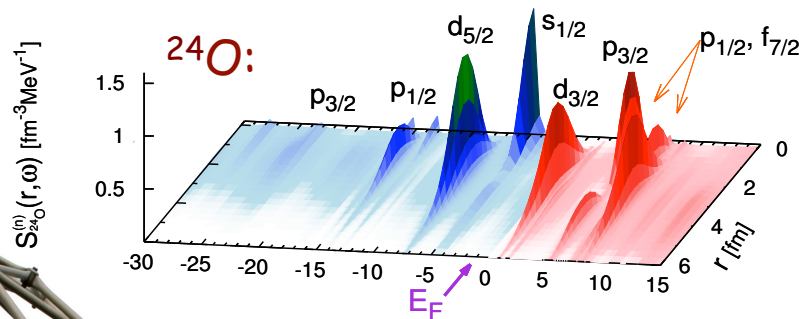
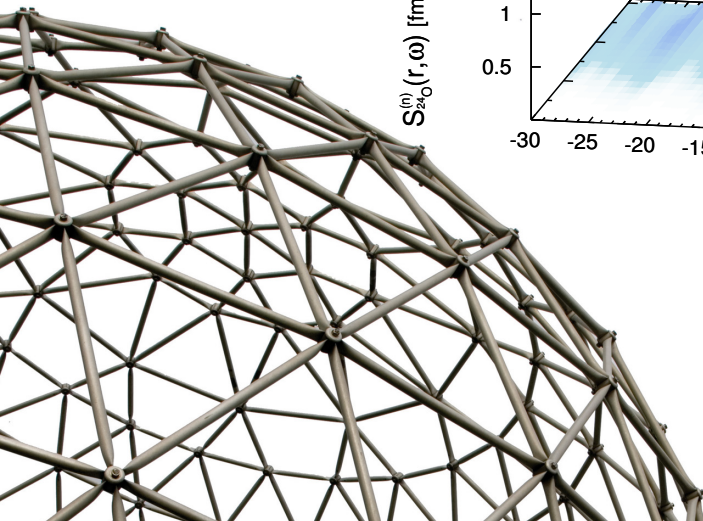


Origin of shell-structure in atomic nuclei

Carlo Barbieri — University of Surrey

17 January 2016



Current Status of low-energy nuclear physics

Composite system of interacting fermions

Binding and limits of stability

Coexistence of individual and collective behaviors

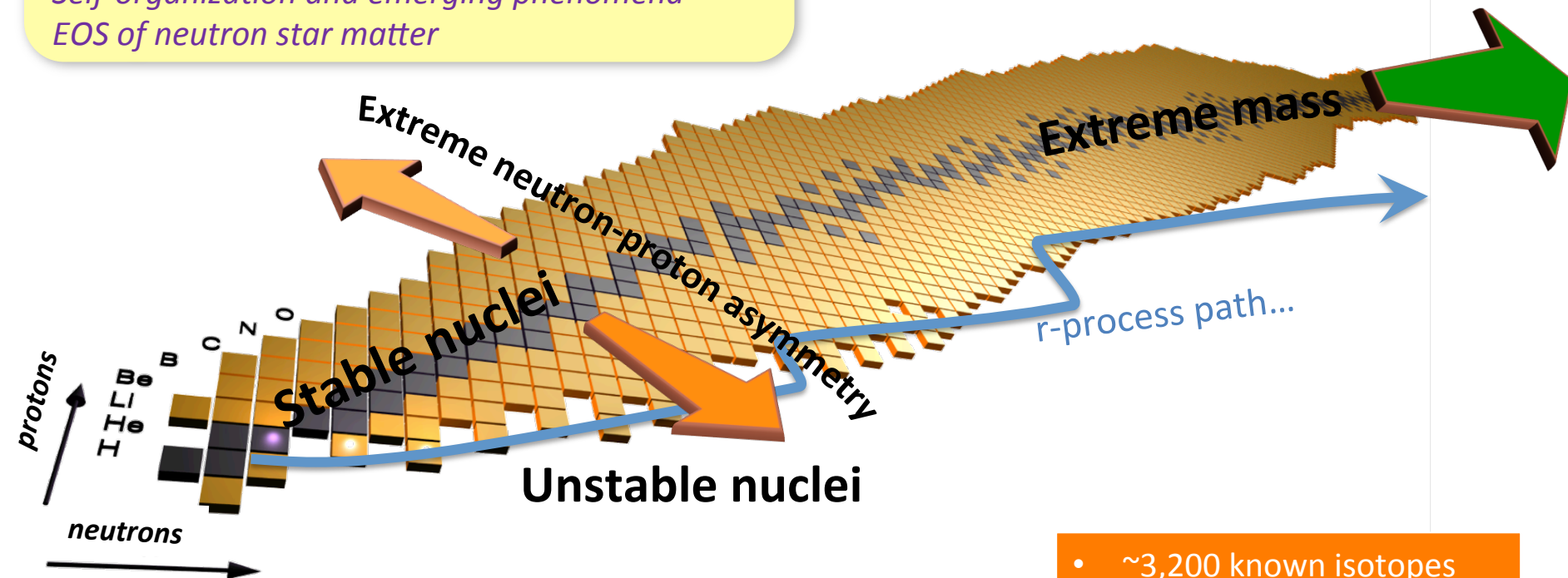
Self-organization and emerging phenomena

EOS of neutron star matter

Experimental

programs

RIKEN, FAIR, FRIB

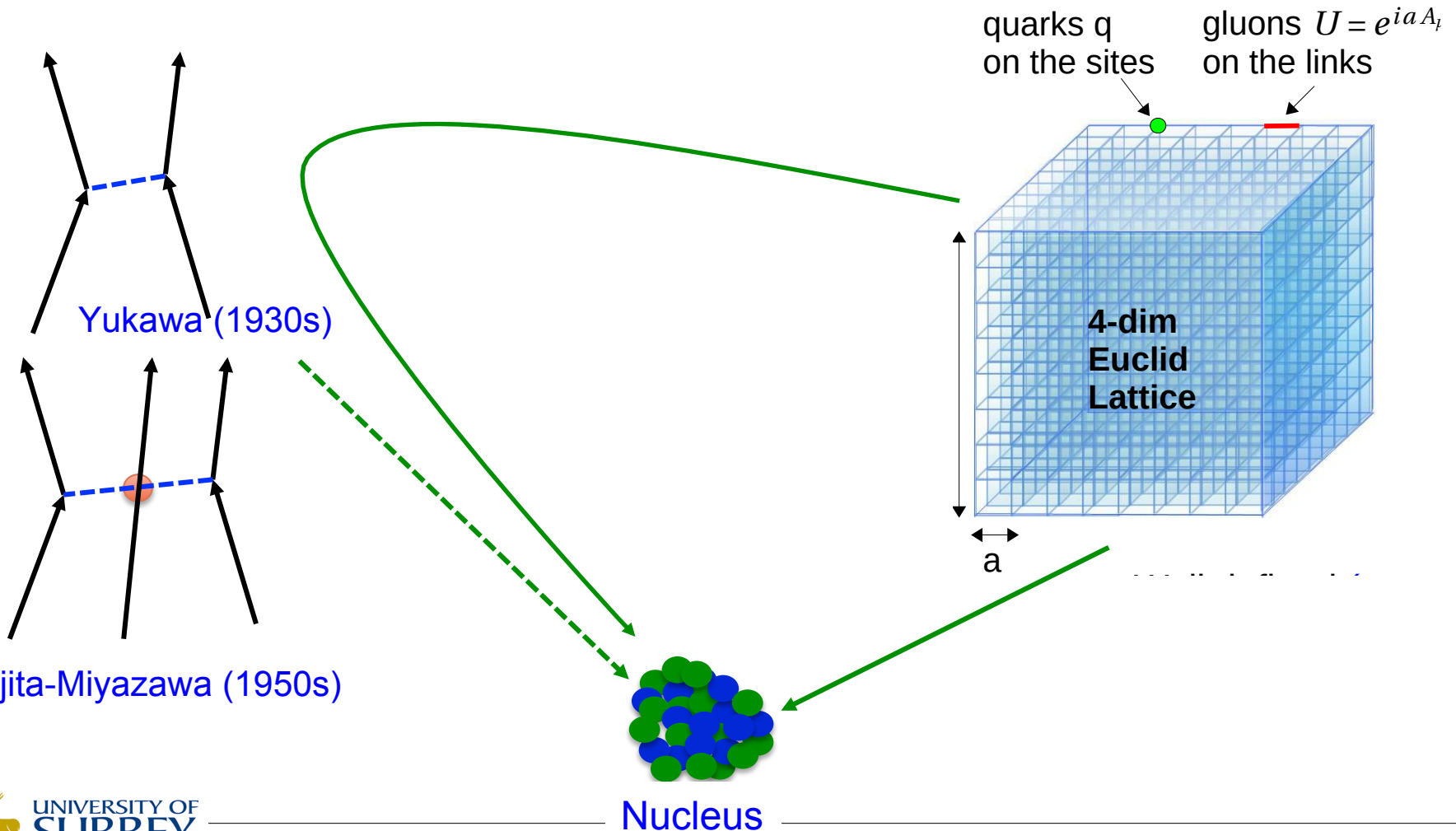


- ~3,200 known isotopes
- ~7,000 predicted to exist
- Correlation characterised in full for ~283 stable

Nature **473**, 25 (2011); **486**, 509 (2012)

Approaches to nuclei from LQCD

$$L = -\frac{1}{4} G_{\mu\nu}^a G_a^{\mu\nu} + \bar{q} \gamma^\mu (i \partial_\mu - g t^a A_\mu^a) q - m \bar{q} q$$

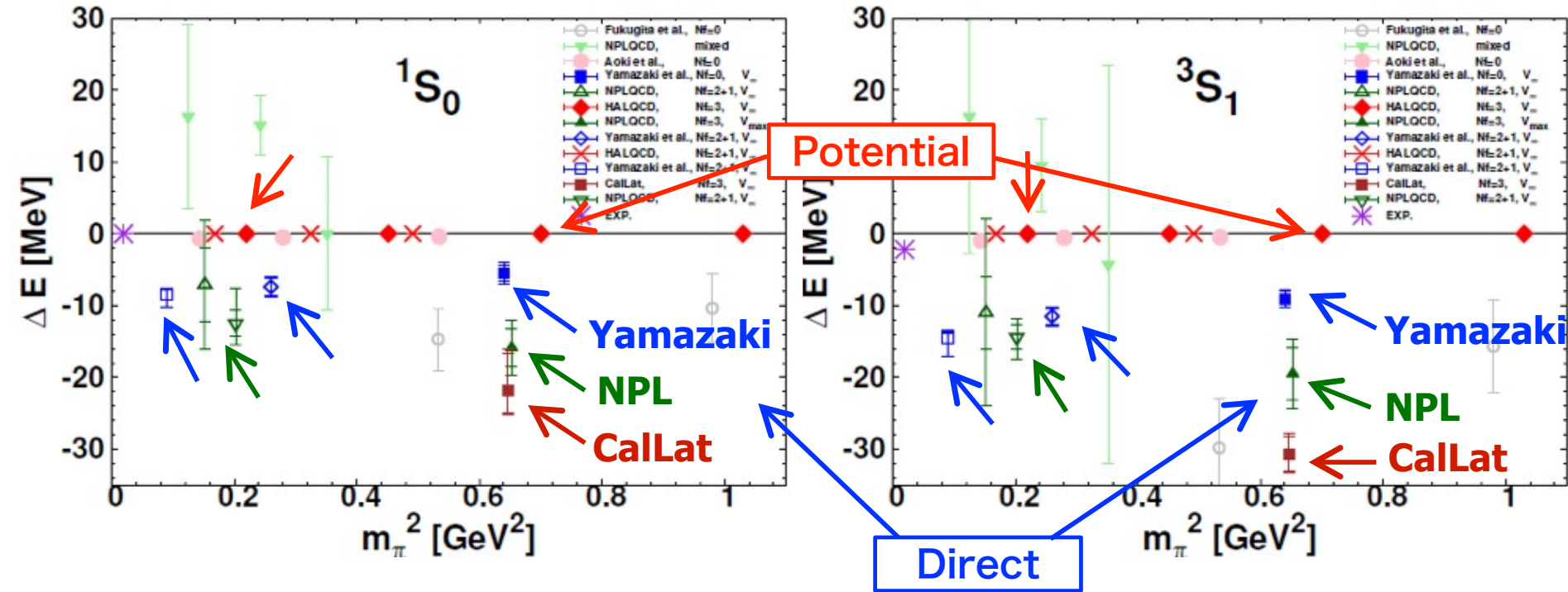


Approaches to nuclei from LQCD

HALQCD coll. -- Talk of **S. Aoki** at Kavli institute, Oct. 2016

“di-neutron”

“deuteron”



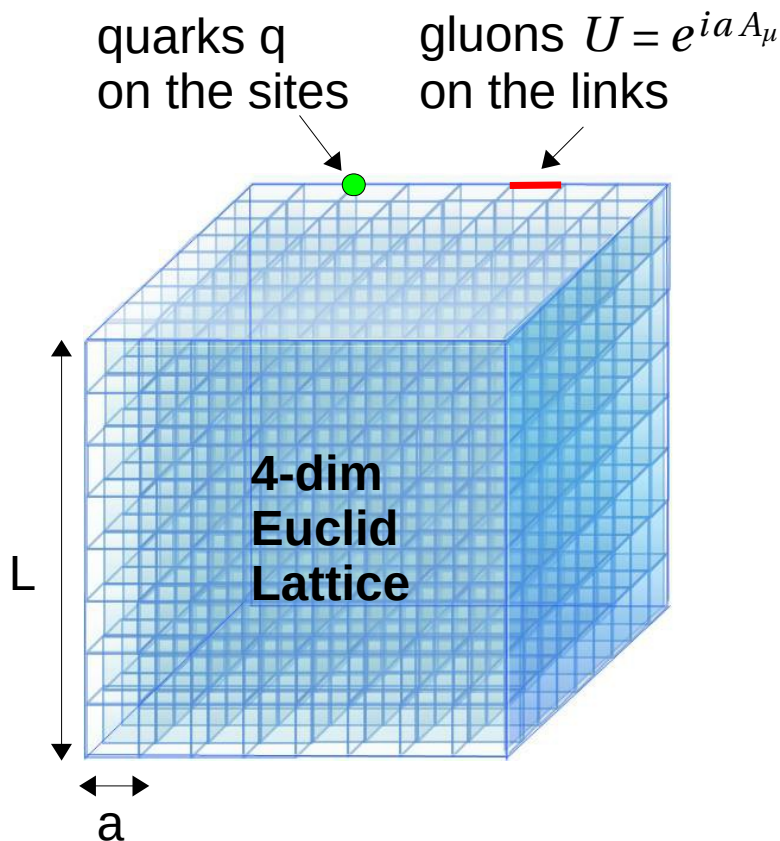
Potential method (HALQCD) :

Direct method (Yamazaki et al./NPL/Callat):

See Z. Davoudi talk on Wednesday!!

Lattice QCD

$$L = -\frac{1}{4} G_{\mu\nu}^a G_a^{\mu\nu} + \bar{q} \gamma^\mu (i \partial_\mu - g t^a A_\mu^a) q - m \bar{q} q$$



Vacuum expectation value

$$\begin{aligned} \langle O(\bar{q}, q, U) \rangle &= \int dU d\bar{q} dq e^{-S(\bar{q}, q, U)} O(\bar{q}, q, U) \\ &= \int dU \det D(U) e^{-S_U(U)} O(\overset{\text{quark propagator}}{D^{-1}(U)}) \\ &= \lim_{N \rightarrow \infty} \frac{1}{N} \sum_{i=1}^N O(D^{-1}(U_i)) \end{aligned}$$

path integral

$\{U_i\}$: ensemble of gauge conf. U
generated w/ probability $\det D(U) e^{-S_U(U)}$

- ★ Well defined (regularized)
- ★ Manifest gauge invariance

- ★ Fully non-perturbative
- ★ Highly predictive

The HAL-QCD Method

Define a general potential $U(\vec{r}, \vec{r}')$ which is **non-local** but **energy independent** up to inelastic threshold, such that:

$$-\frac{\nabla^2}{2\mu} \varphi_{\vec{k}}(\vec{r}) + \int d\vec{r}' U(\vec{r}, \vec{r}') \varphi_{\vec{k}}(\vec{r}') = E_{\vec{k}} \varphi_{\vec{k}}(\vec{r})$$

for the **Nambu-Bethe-Salpeter (NBS)** wave function,

$$\varphi_{\vec{k}}(\vec{r}) = \sum \langle 0 | B_i(\vec{x} + \vec{r}, t) B_j(\vec{x}, t) | B = 2, \vec{k} \rangle$$

Operationally, measure the **4-pt function** on the QCD Lattice

$$\psi(\vec{r}, t) = \sum_{\vec{x}} \langle 0 | B_i(\vec{x} + \vec{r}, t) B_j(\vec{x}, t) J(t_0) | 0 \rangle = \sum_{\vec{k}} A_{\vec{k}} \varphi_{\vec{k}}(\vec{r}) e^{-W_{\vec{k}}(t-t_0)} + \dots$$

and extract $U(\vec{r}, \vec{r}')$ from:

$$\left\{ 2M_B - \frac{\nabla^2}{2\mu} \right\} \psi(\vec{r}, t) + \int d\vec{r}' U(\vec{r}, \vec{r}') \psi(\vec{r}', t) = -\frac{\partial}{\partial t} \psi(\vec{r}, t)$$

A **local potential** $V(\vec{r})$ is then obtained through a derivative expansion of $U(\vec{r}, \vec{r}')$, which **must give the same observables** of the LQCD simulation:

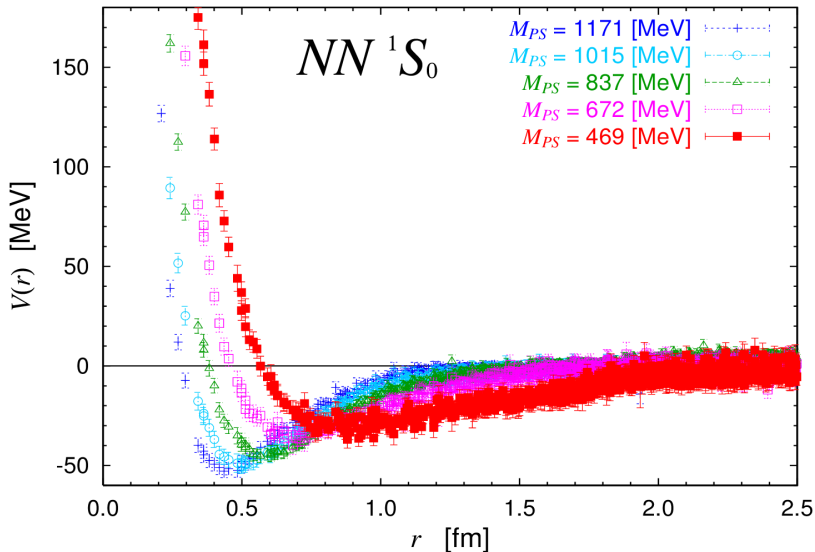
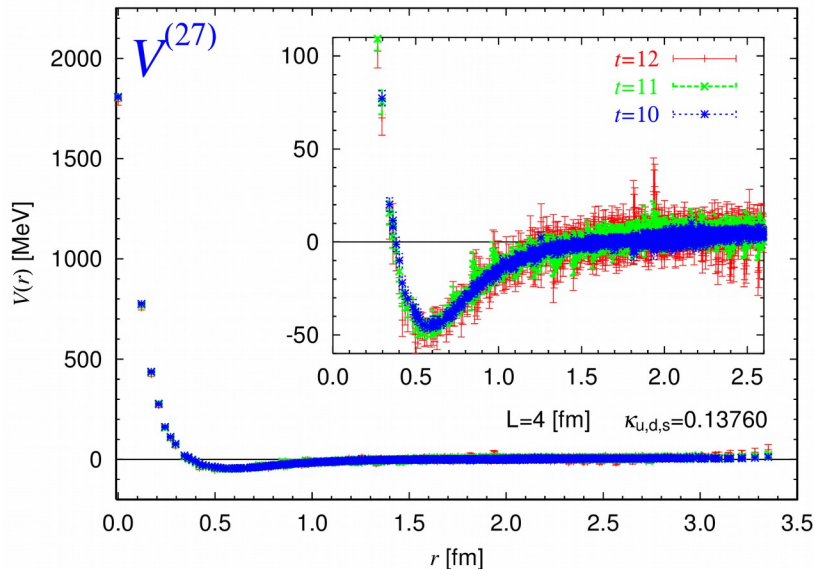
$$U(\vec{r}, \vec{r}') = \delta(\vec{r} - \vec{r}') V(\vec{r}, \nabla) = \delta(\vec{r} - \vec{r}') \{ V(\vec{r}) + \mathcal{O}(\nabla) + \mathcal{O}(\nabla^2) + \dots \}$$

$$\rightarrow V(\vec{r}) = \frac{1}{2\mu} \frac{\nabla^2 \psi(\vec{r}, t)}{\psi(\vec{r}, t)} - \frac{\frac{\partial}{\partial t} \psi(\vec{r}, t)}{\psi(\vec{r}, t)} - 2M_B$$

Tensor/Yukawa
force in S-D

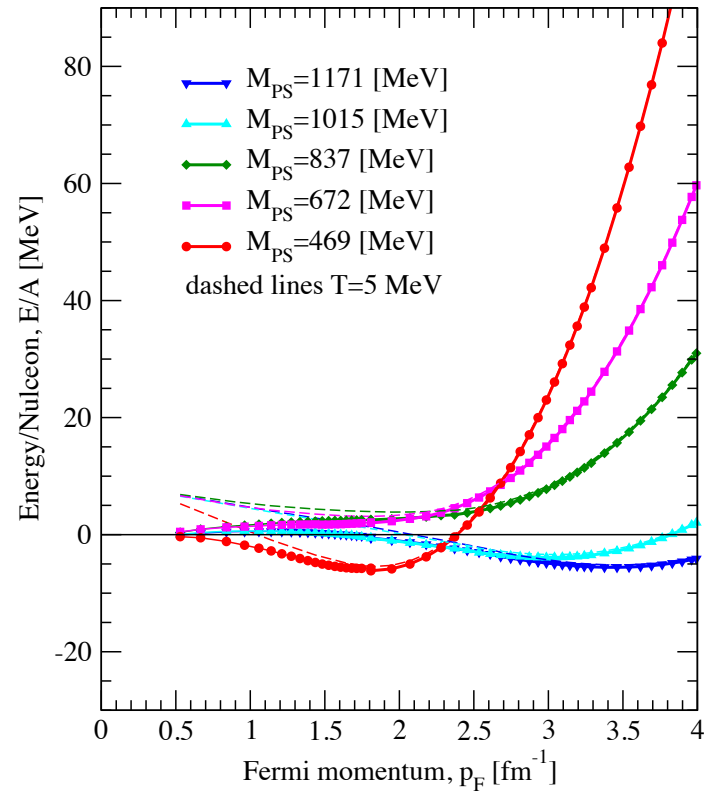
Spin-orbit
force, P waves

Two-Nucleon HAL potentials



Quark mass dependence of $V(r)$ for NN partial wave (1S_0 , 3S_1 , 3S_1 - 3D_1)

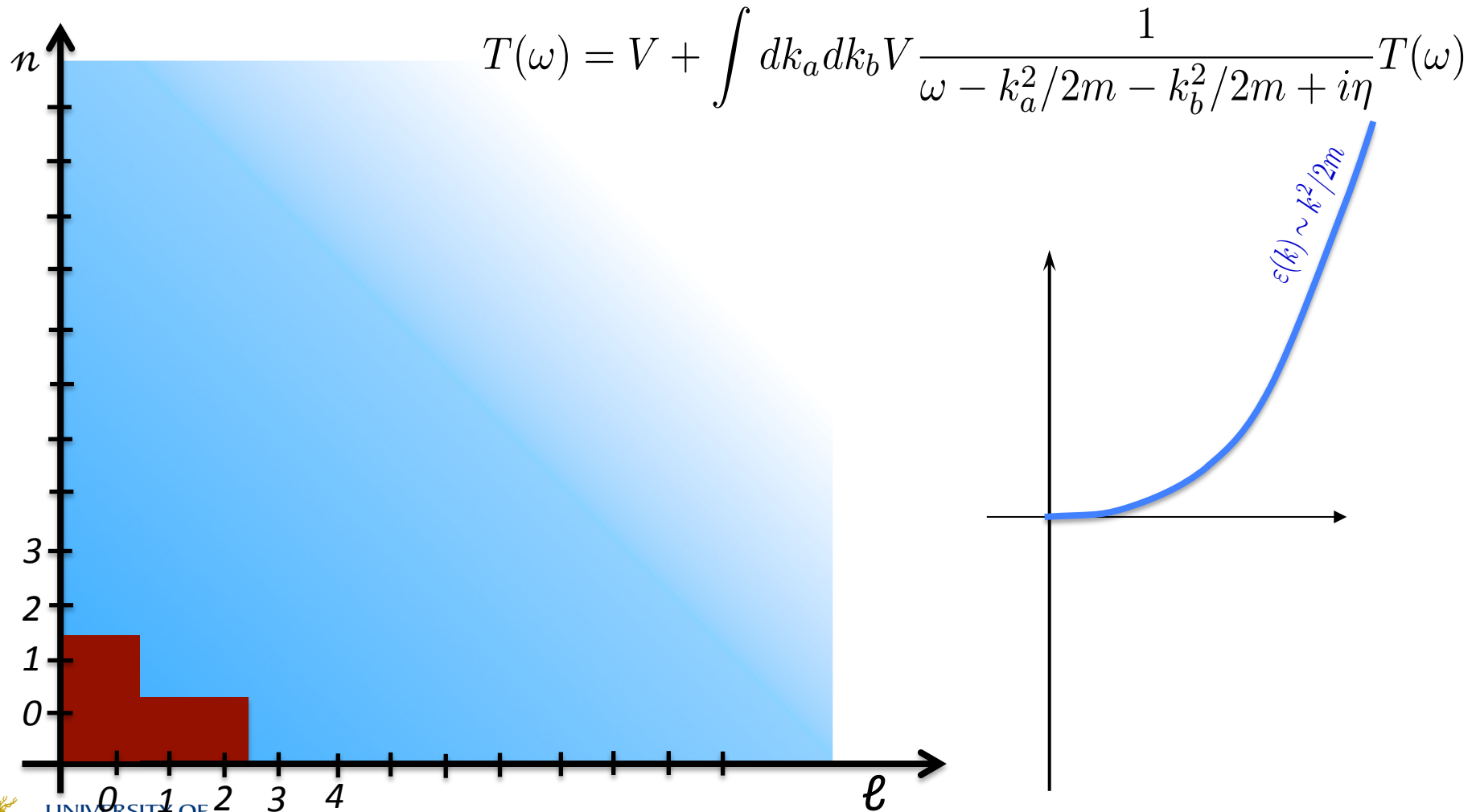
→ Potentials become stronger m_π as decreases.



T. Inoue *et al.*,
Phys. Rev. Lett. **111** 112503 (2013).

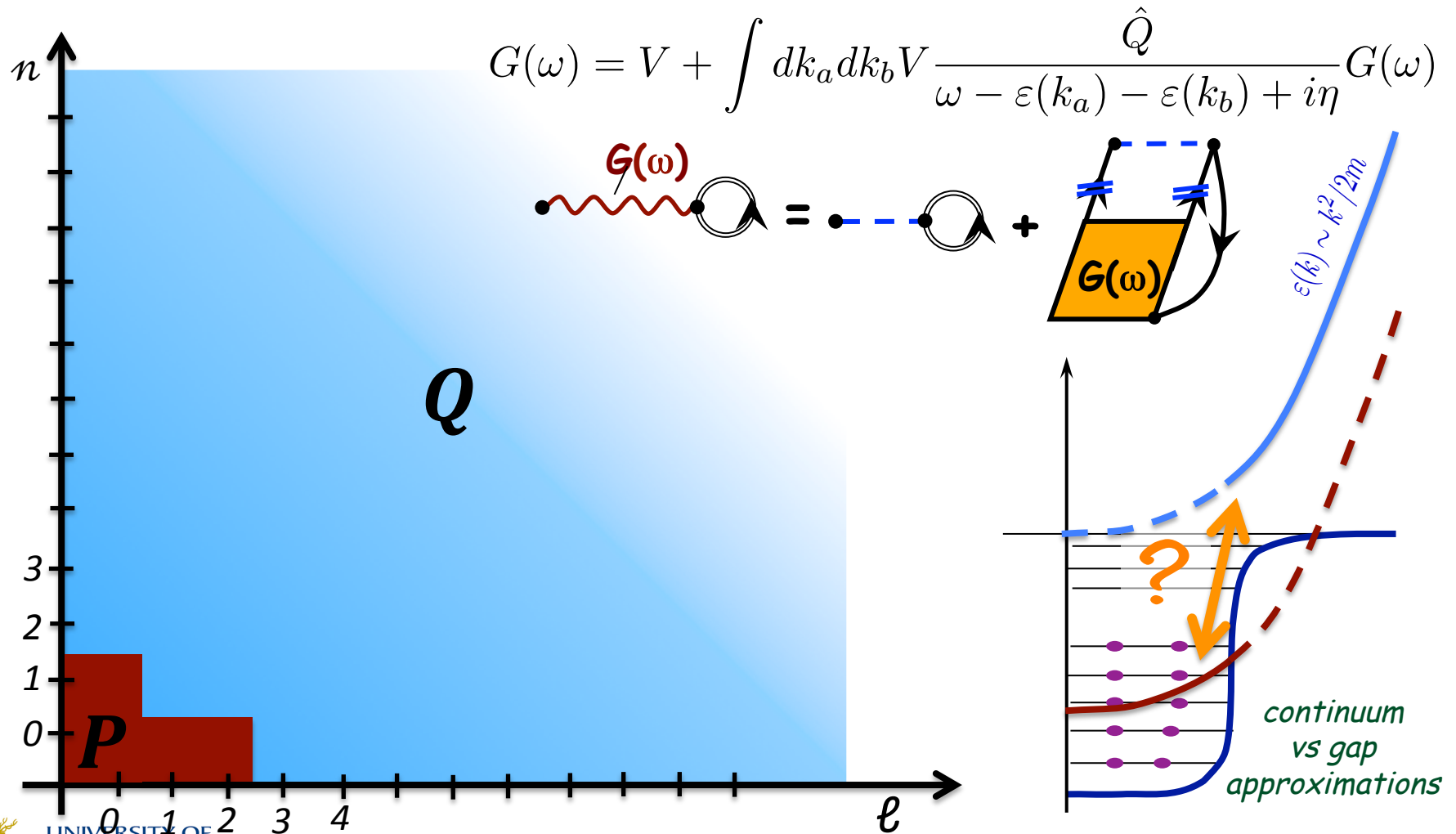
Analysis of Brueckner HF

Scattering of two nucleon in free space:



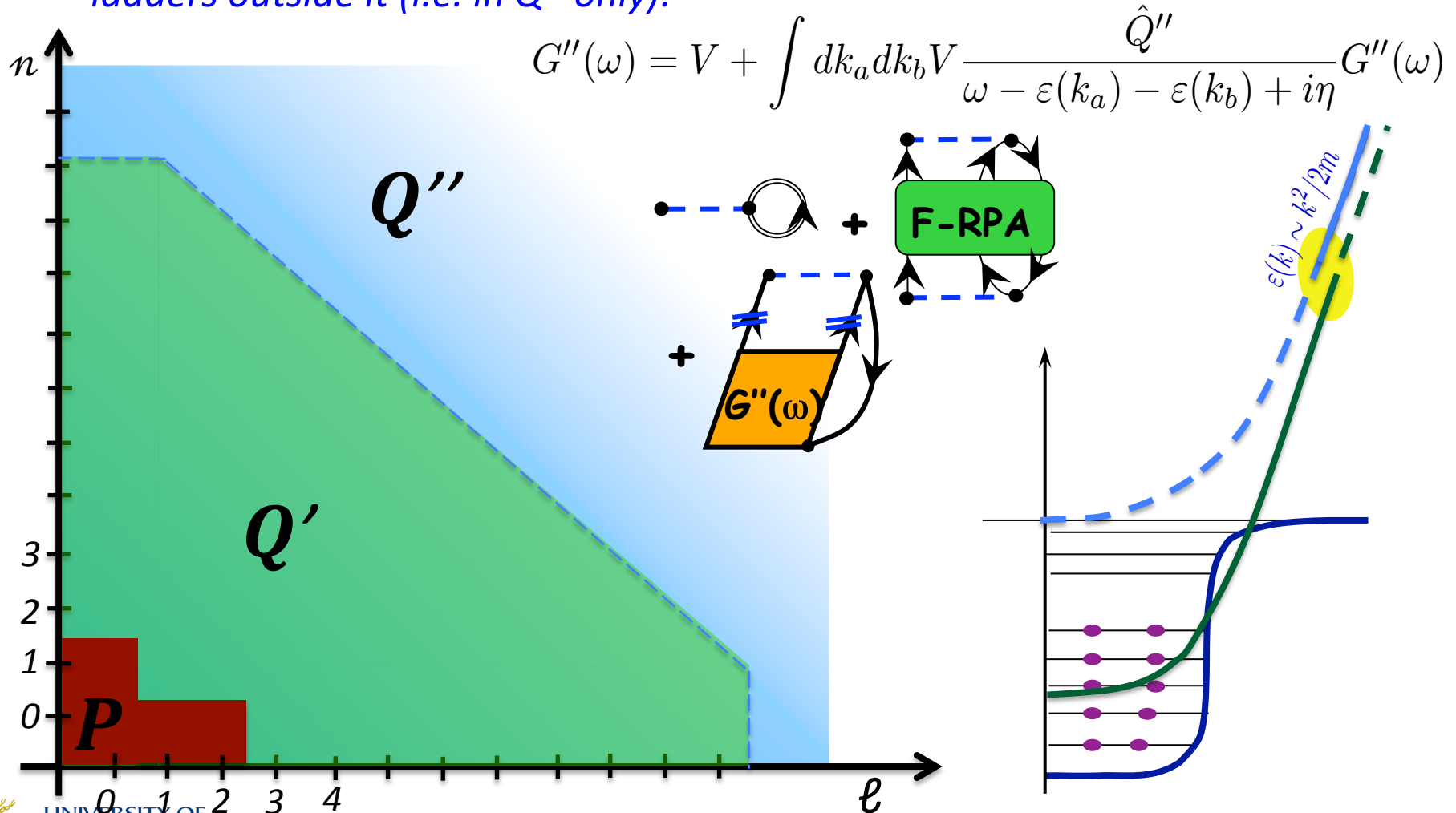
Analysis of Brueckner HF

Scattering of two nucleons outside the Fermi sea (\rightarrow BHF):



Mixed SCGF-Brueckner approach

Solve full many-body dynamics in model space ($P+Q'$) and the Goldstone's ladders outside it (i.e. in Q'' only):



Treating short-range corr. with a G-matrix

- The short-range core can be treated by summing ladders outside the model space:

$$\Sigma_{\alpha\beta}^{\text{MF}}(\omega) = i \sum_{\gamma\delta} \int \frac{d\omega'}{2\pi} G_{\alpha\gamma, \delta\beta}(\omega + \omega') g_{\delta\gamma}(\omega') = \text{diagram}$$

The diagram shows a red wavy line labeled $G(\omega)$ connecting two black dots. The right dot is part of a self-energy loop (a circle with an arrow).

$$\Sigma^*(\mathbf{r}, \mathbf{r}'; \omega) = \Sigma^{\text{MF}}(\mathbf{r}, \mathbf{r}'; \omega) + \tilde{\Sigma}(\mathbf{r}, \mathbf{r}'; \omega).$$

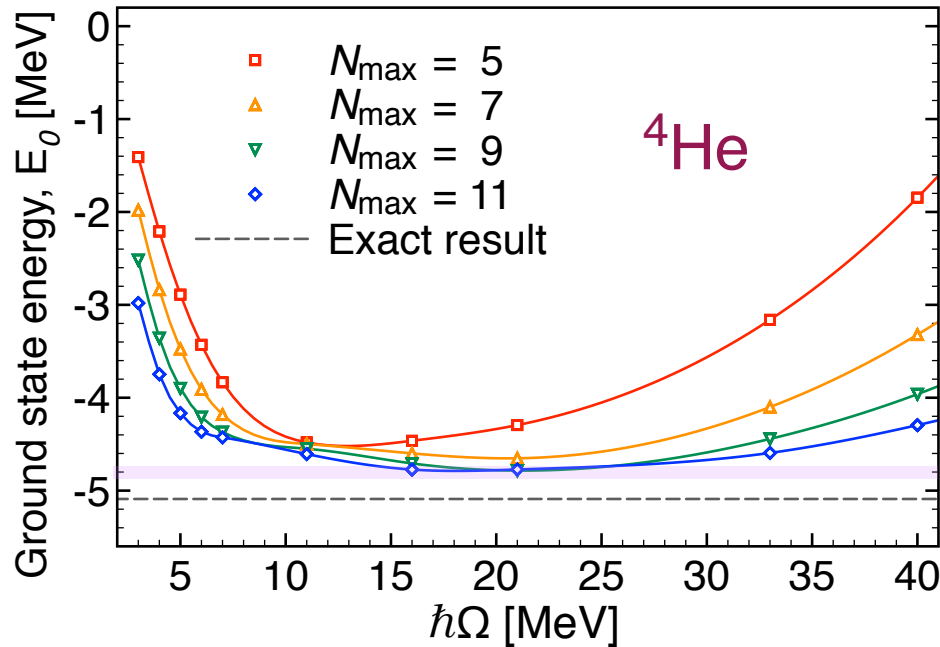
$$Z_\alpha = \int d\mathbf{r} |\psi_\alpha^{A\pm 1}(\mathbf{r})|^2 = \frac{1}{1 - \left. \frac{\partial \Sigma_{\hat{a}\hat{a}}^*(\omega)}{\partial \omega} \right|_{\omega = \pm(E_\alpha^{A\pm 1} - E_0^A)}}$$

Two contributions to the derivative:

- $\Sigma_{\alpha\beta}^{\text{MF}}(\omega)$ is due to scattering to (high-k) states in the Q space
- $\Sigma(\mathbf{r}, \mathbf{r}'; \omega)$ accounts for low-energy (long range) correlations

Benchmark on ^4He

C. McIlroy, CB, et al., arXiv:1701.02607 [nucl-th]

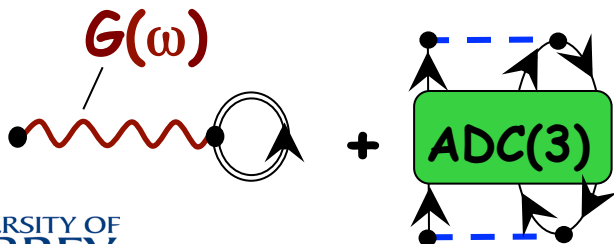


Can benchmark the $G_{\text{mtx}} + \text{ADC}(3)$ method on light ^4He , where exact solutions are possible:

	$G(\omega) + \text{ADC}(3)$	Exact
HALQCD @ $m_\pi \approx 470 \text{ MeV}$	4.79(3) MeV	5.09 MeV ¹

¹H. Nemura *et al.*, Int. J. Mod. Phys. E **23**, 1461006 (2014)

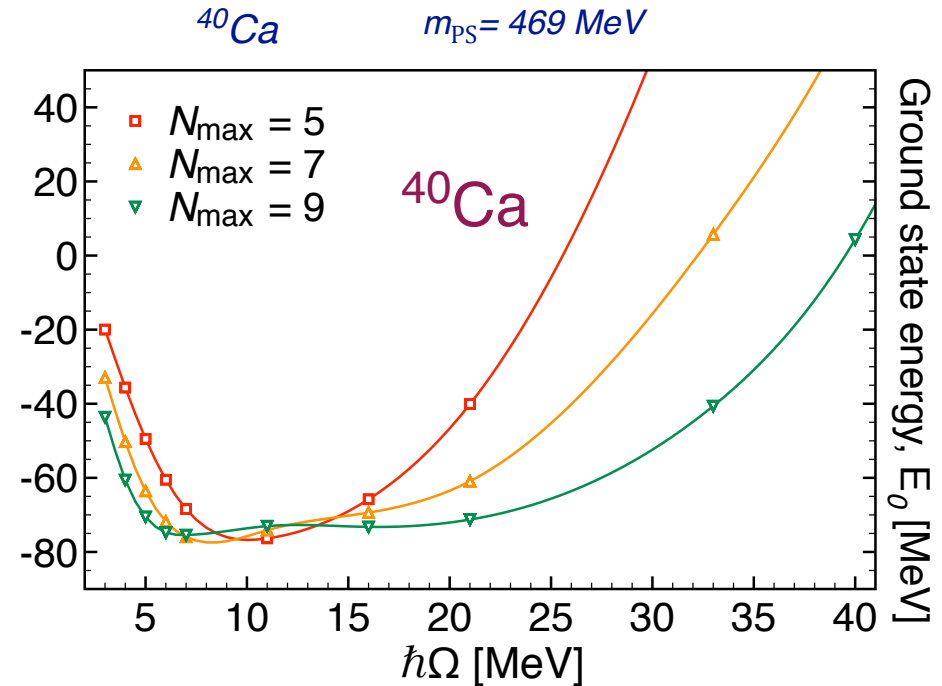
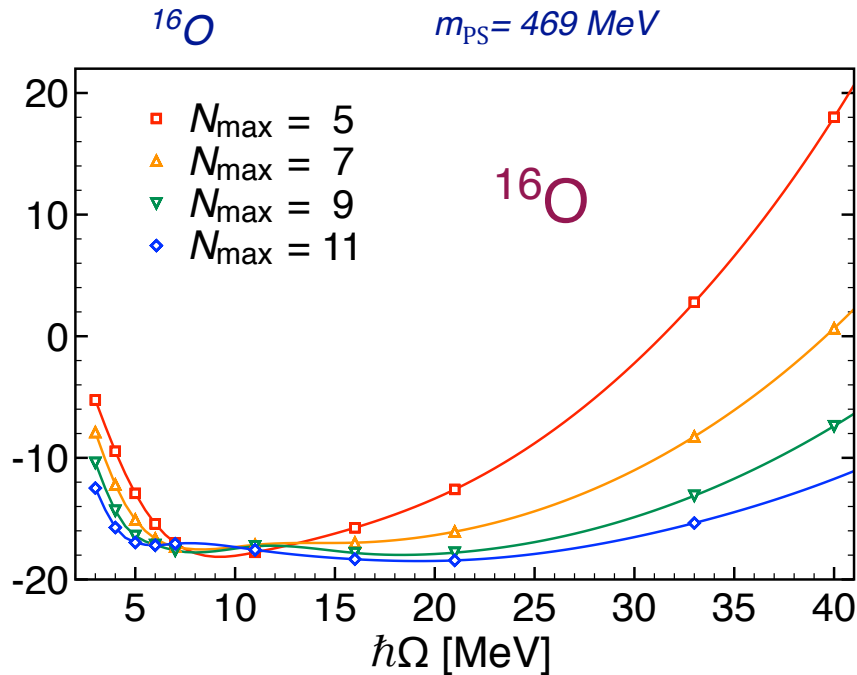
→ Can expect accuracy on binding energies at about 10%



$$G''(\omega) = V + \int dk_a dk_b V \frac{\hat{Q}''}{\omega - \varepsilon(k_a) - \varepsilon(k_b) + i\eta} G''(\omega)$$

Binding of ^{16}O and ^{40}Ca :

C. McIlroy, CB, et al., arXiv:1701.02607 [nucl-th]



Binding energies are $\sim 17 \text{ MeV}$ ^{16}O and $70\text{--}75 \text{ MeV}$ for ^{40}Ca . Possibly being underestimated by 10%

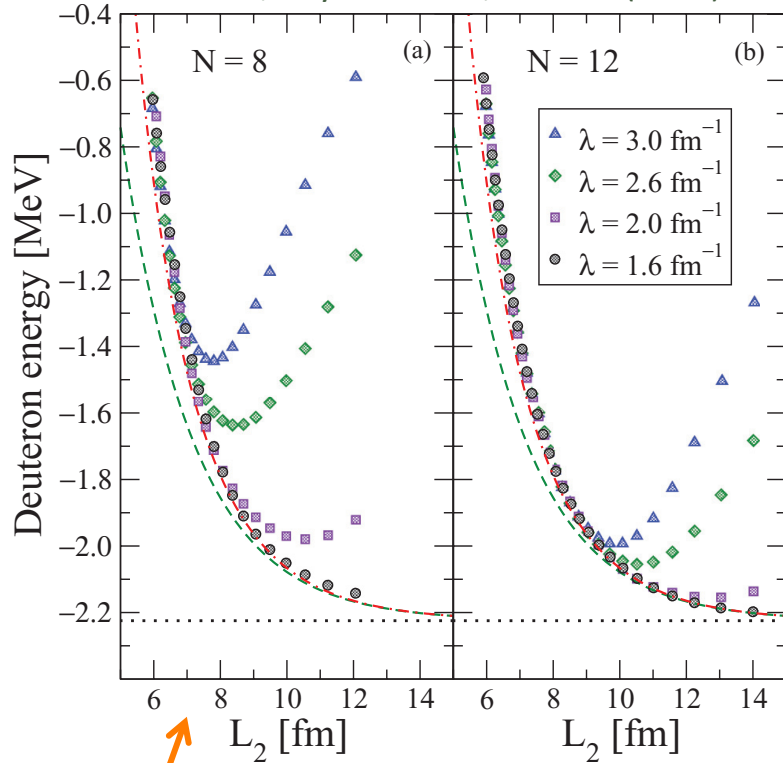
→ ^{16}O at $m_{\pi} \approx 470 \text{ MeV}$ is unstable toward $4\text{-}\alpha$ breakup!

E_0^A [MeV]	^4He	^{16}O	^{40}Ca
BHF [22]	-8.1	-34.7	-112.7
$G(\omega) + \text{ADC}(3)$	-4.80(0.03)	-17.9 (0.3) (1.8)	-75.4 (6.7) (7.5)
Exact Result [51]	-5.09	—	—
Separation into ^4He clusters:		-2.46 (0.3) (1.8)	24.5 (6.7) (7.5)

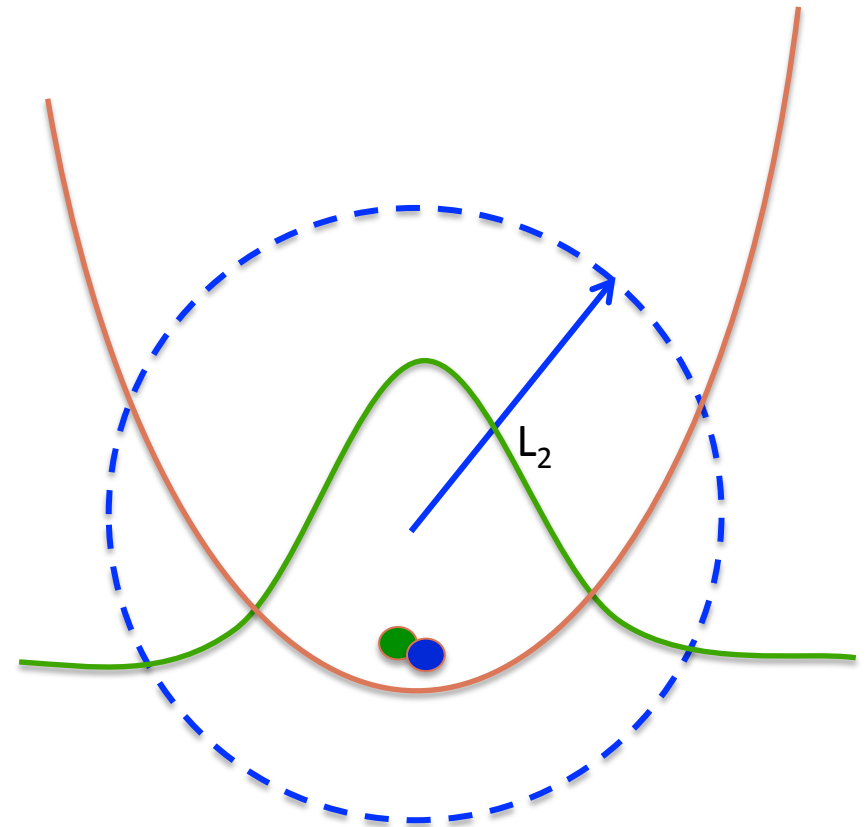
[C.S. McIlroy, CB, HAL coll., in prep]

Infrared convergence

Moore et al., Phys. Rev. C **87**, 044326 (2013)

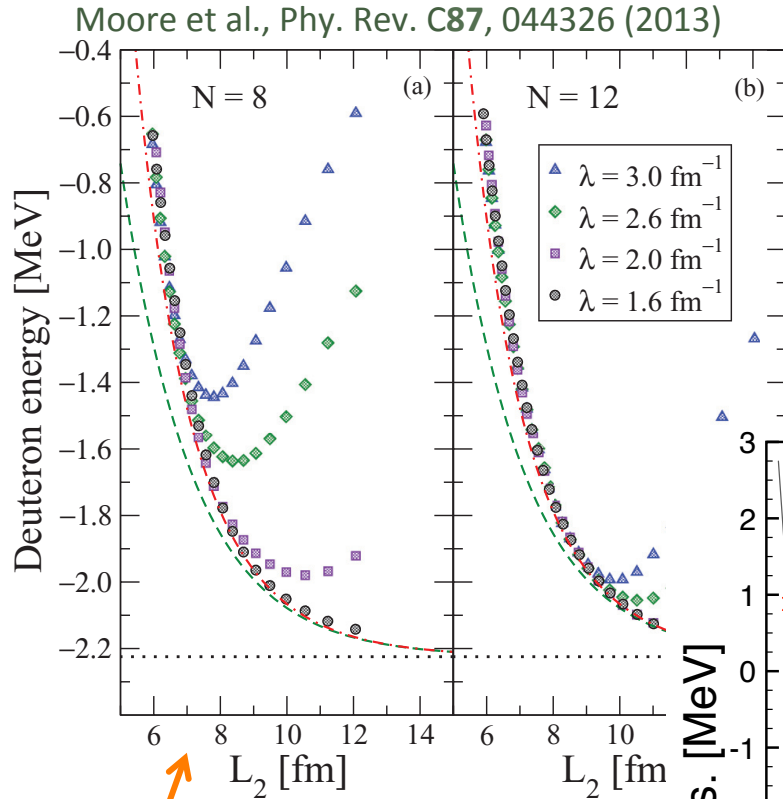


Deuteron g.s. Energy
EM(500) – N3LO two-nucleon force

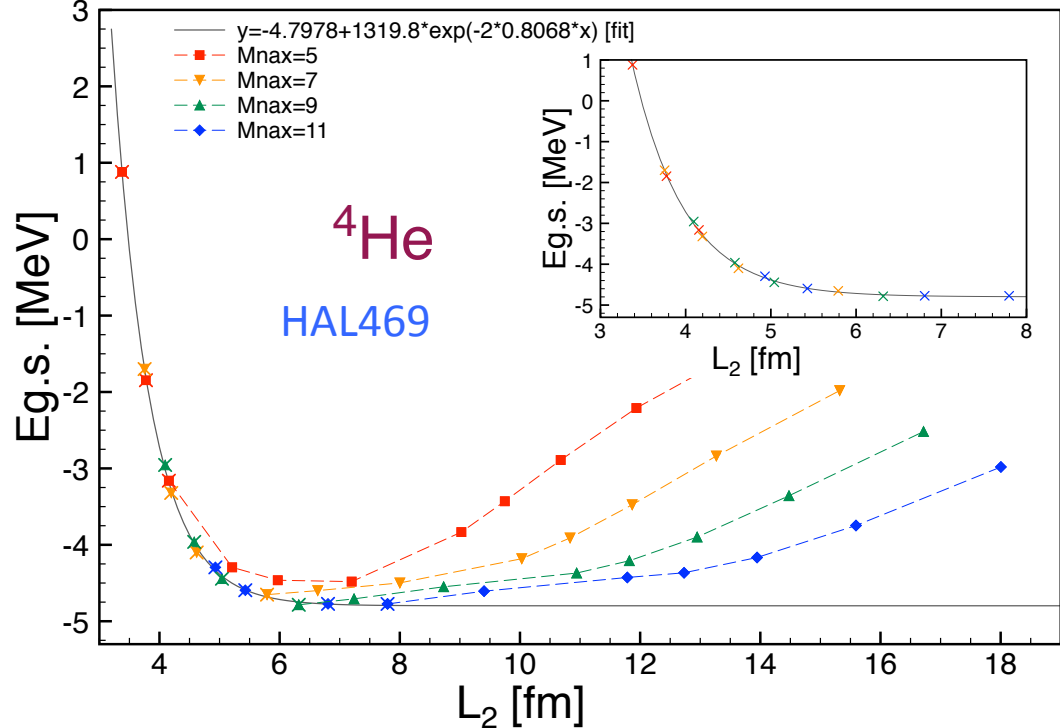
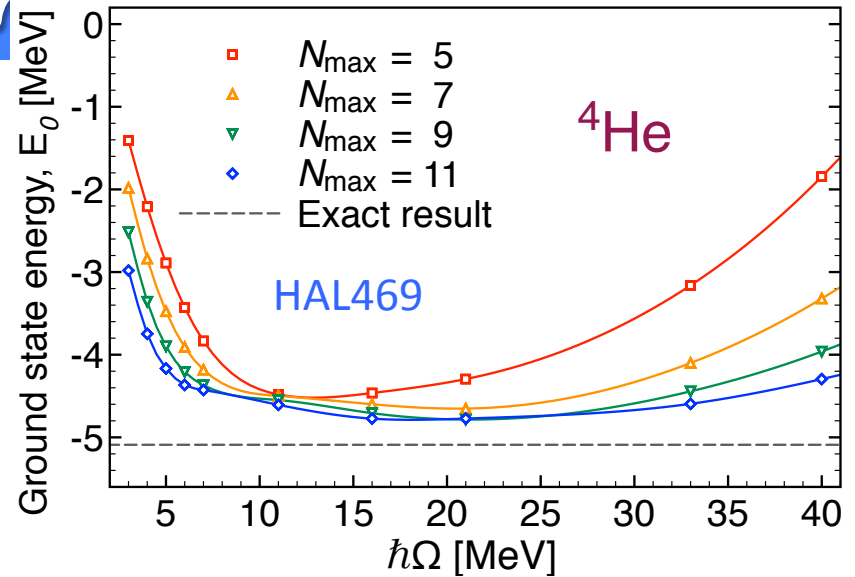


$$L_2 = \sqrt{2(N + 3/2 + 2)}b$$

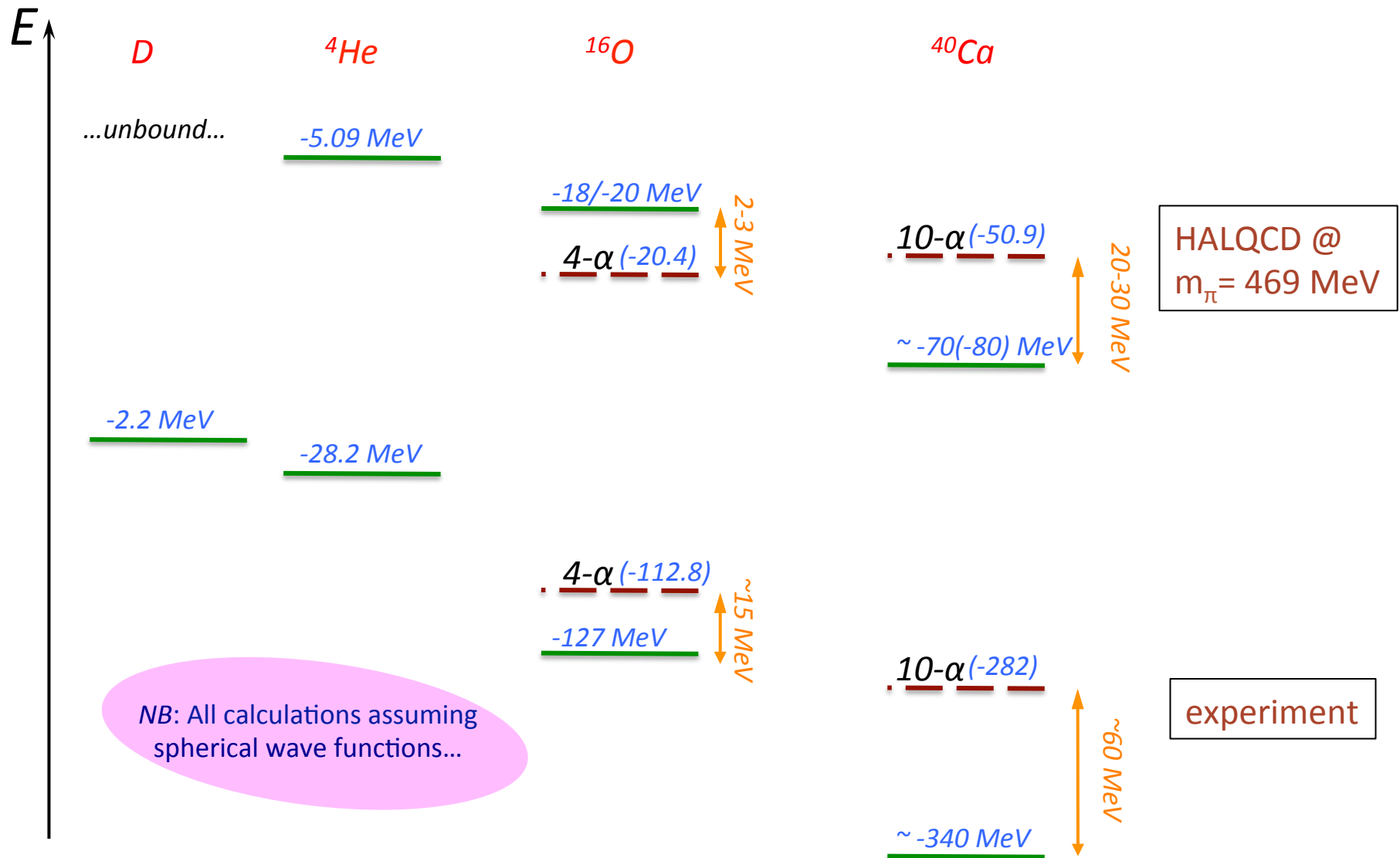
Infrared convergence



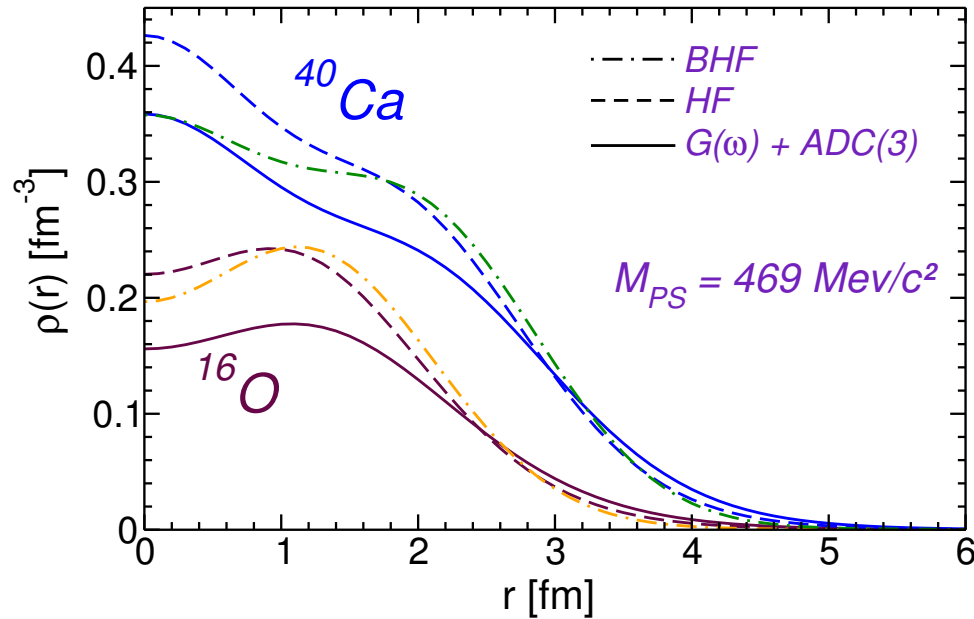
Deuteron g.s. Energy
EM(500) – N3LO two-nuc



Results for binding



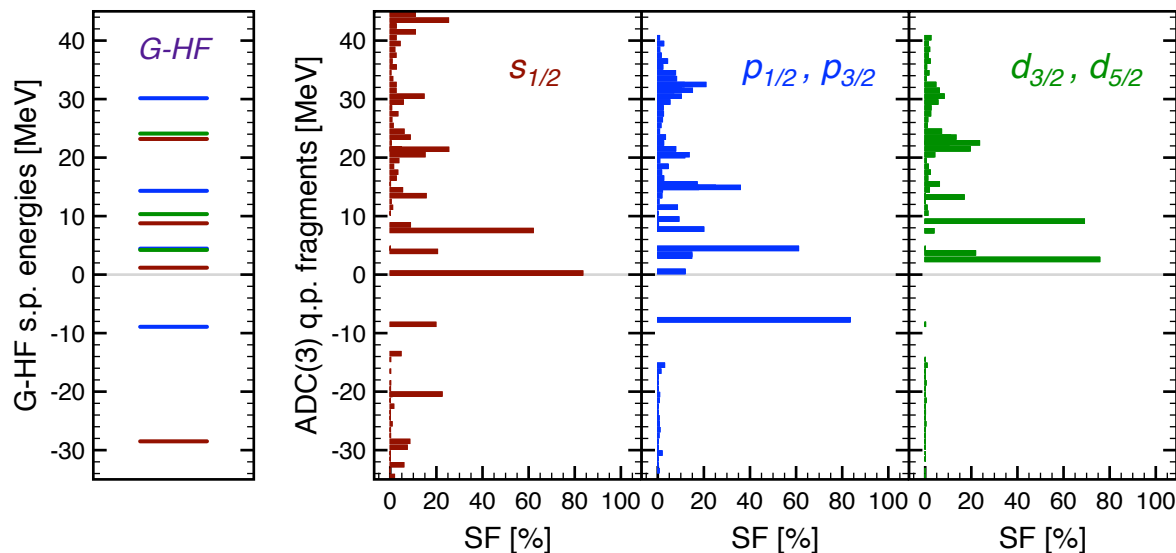
Matter distribution of ^{16}O and ^{40}Ca :



Calculated matter radii at $m_\pi \approx 470 \text{ MeV}$:

		^{16}O	^{40}Ca
$r_{pt\text{-matter}}$:	BHF [22]	2.35 fm	2.78 fm
	HF	2.39 fm	2.78 fm
	$G(\omega) + \text{ADC}(3)$	2.64 fm	2.97 fm
r_{charge} :	$G(\omega) + \text{ADC}(3)$	2.77 fm	3.08 fm
	Experiment [54, 55]	2.73 fm	3.48 fm

Spectral strength in ^{16}O and ^{40}Ca :

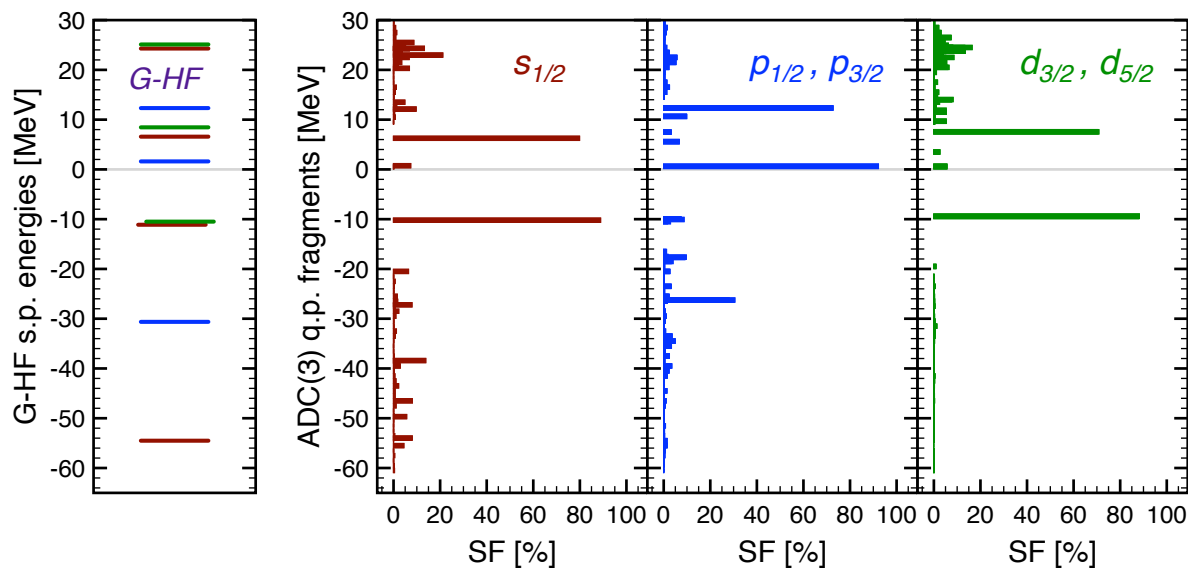


Particle-hole gaps:

^{16}O

$m_\pi = 469 \text{ MeV}$: $\sim 8 \text{ MeV}$

Expt (phys m_π): 11.5 MeV

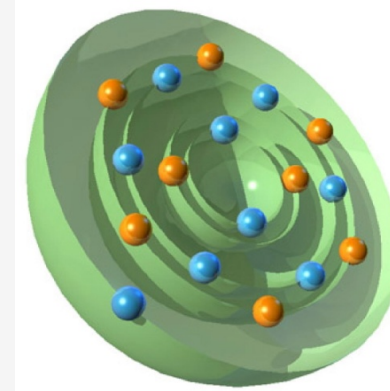
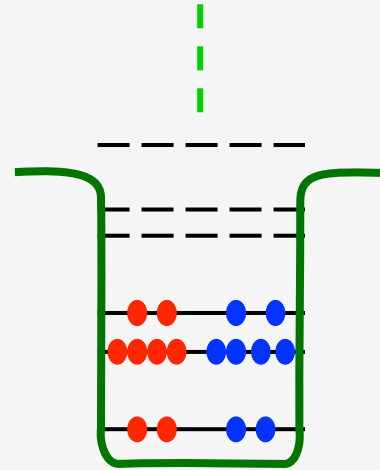
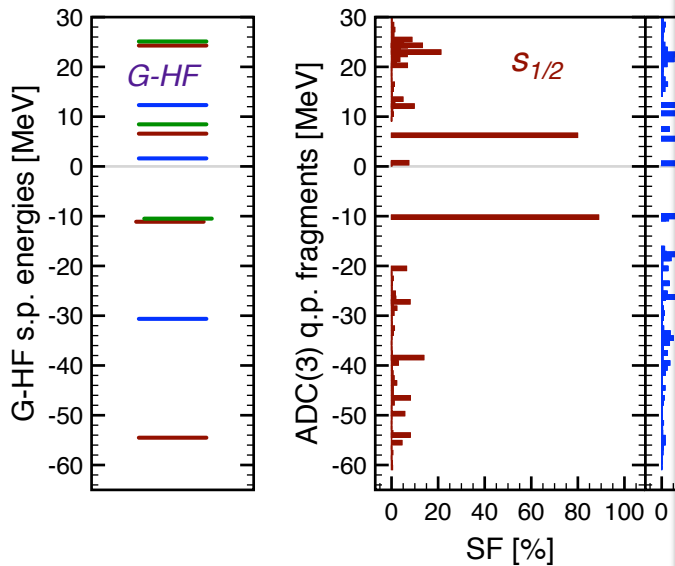
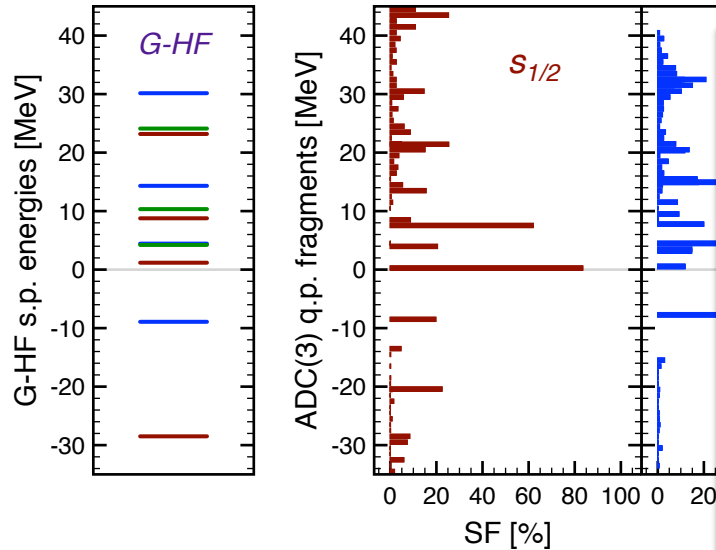


^{40}Ca

$m_\pi = 469 \text{ MeV}$: $\sim 10 \text{ MeV}$

Expt (phys m_π): 7.5 MeV

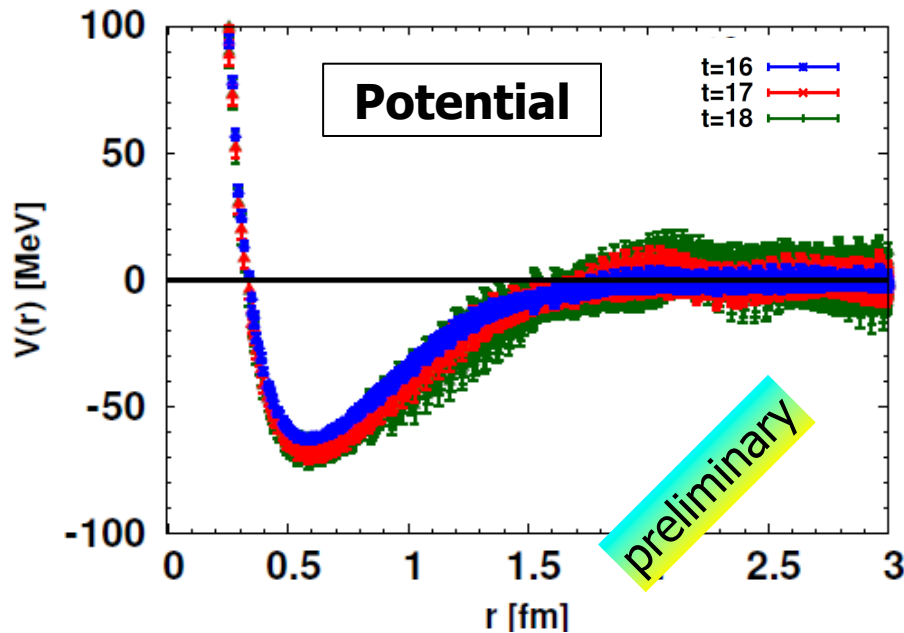
Spectral strength in ^{16}O and ^{40}Ca :



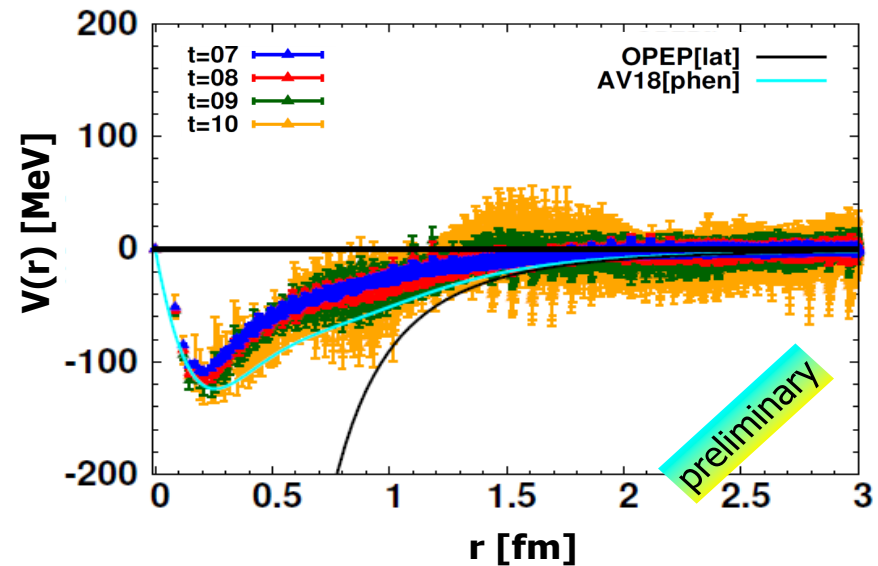
Future application for Y s in nuclei now possible

- Physical mass now under reach ($m_\pi \approx 145$ MeV) for hyperons
- Need to improve on statistic for the NN sector

$\Omega\Omega$ potential



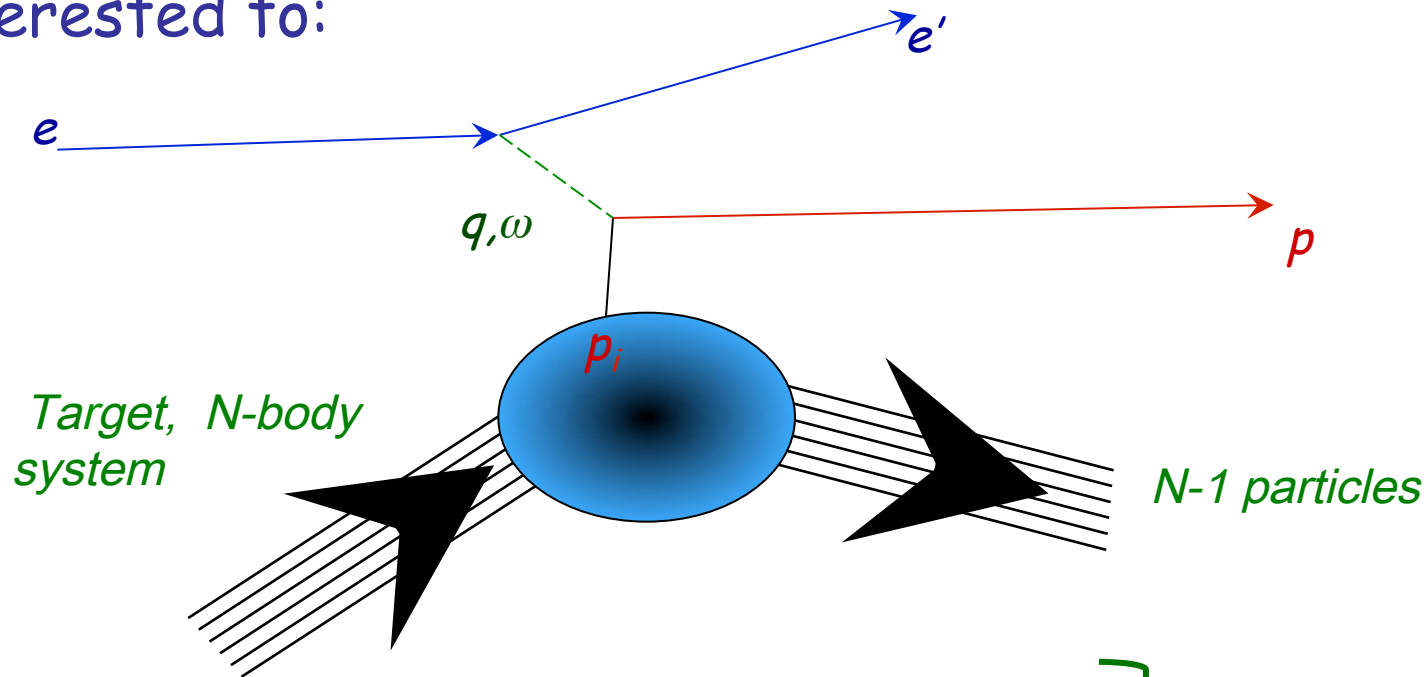
$NN(^3S_1)$ tensor potential



HALQCD coll. -- Talk of **S. Aoki** at Kavli institute, Oct. 2016

Spectroscopy via knock out reactions - *basic idea*

Use a probe (ANY probe) to eject the particle we are interested to:



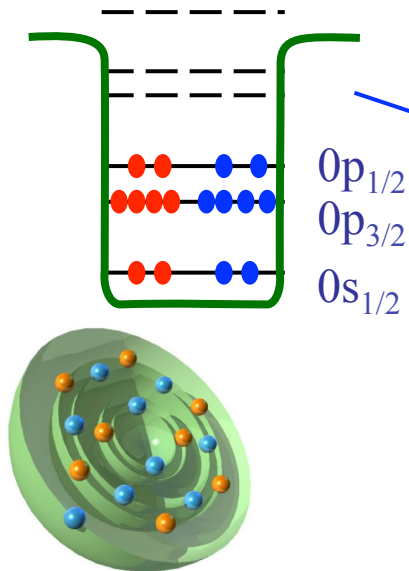
Basic idea:

- we know, e , e' and p
- "get" *energy and momentum of p_i* :
$$p_i = k_e' + k_p - k_e$$
$$E_i = E_e' + E_p - E_e$$

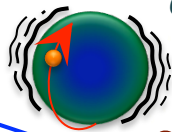
Better to choose
large transferred
momentum and weak
probes!!!

Concept of correlations

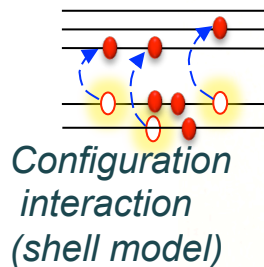
independent
particle picture



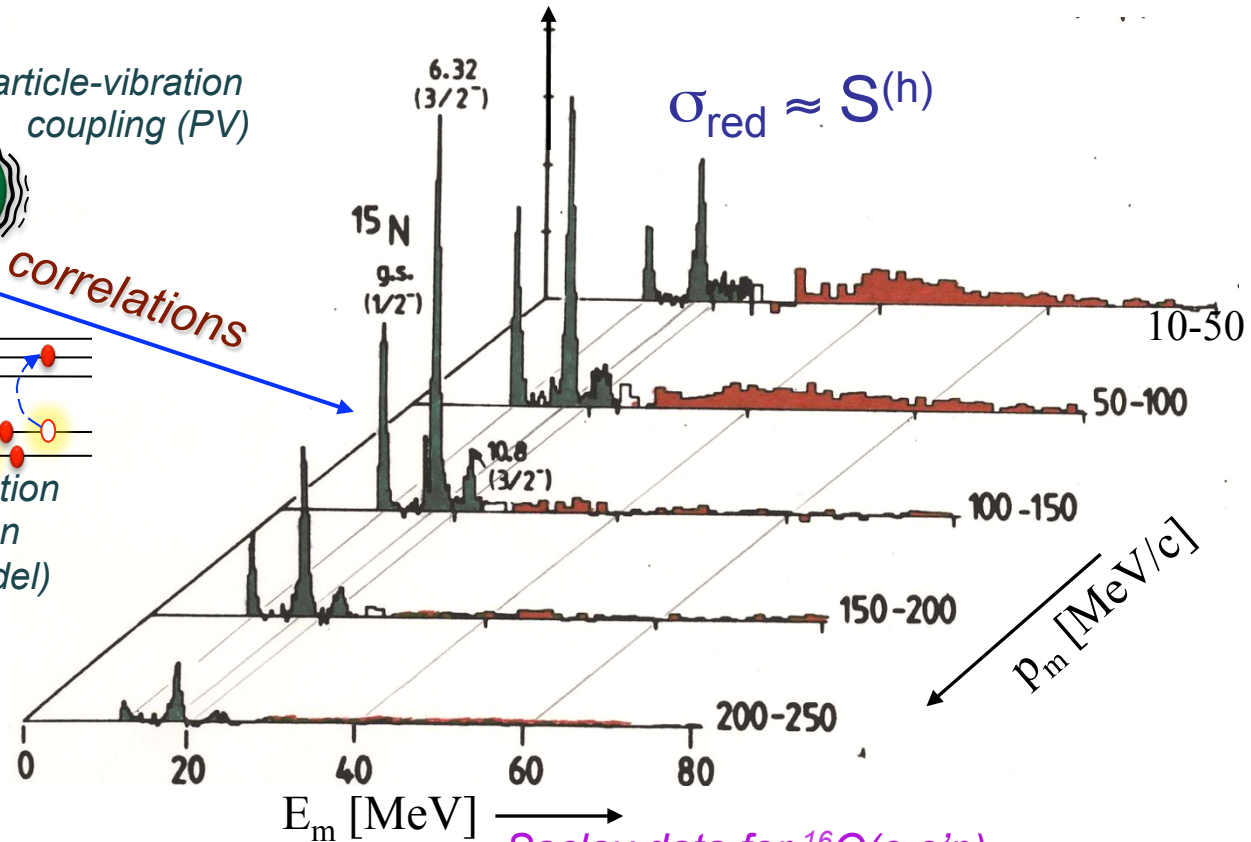
Particle-vibration
coupling (PV)



correlations



Spectral function: distribution of
momentum (p_m) and energies (E_m)



Saclay data for $^{16}\text{O}(e,e'p)$

[Mougey et al., Nucl. Phys. A335, 35 (1980)]

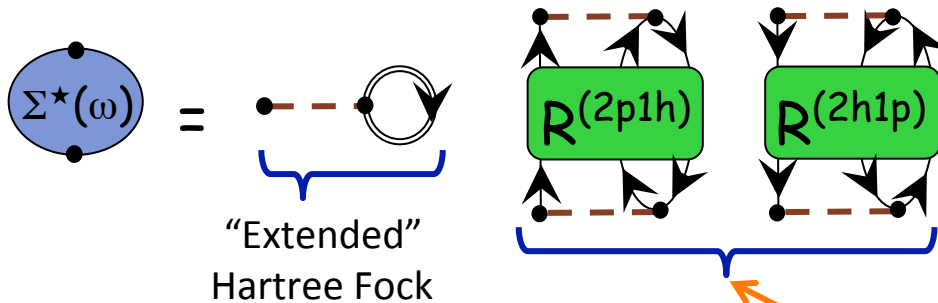
Understood for a few stable closed shells:

[CB and W. H. Dickhoff, Prog. Part. Nucl. Phys 52, 377 (2004)]

The FRPA Method in Two Words

Particle vibration coupling is the main cause driving the distribution of particle strength—on both sides of the Fermi surface...

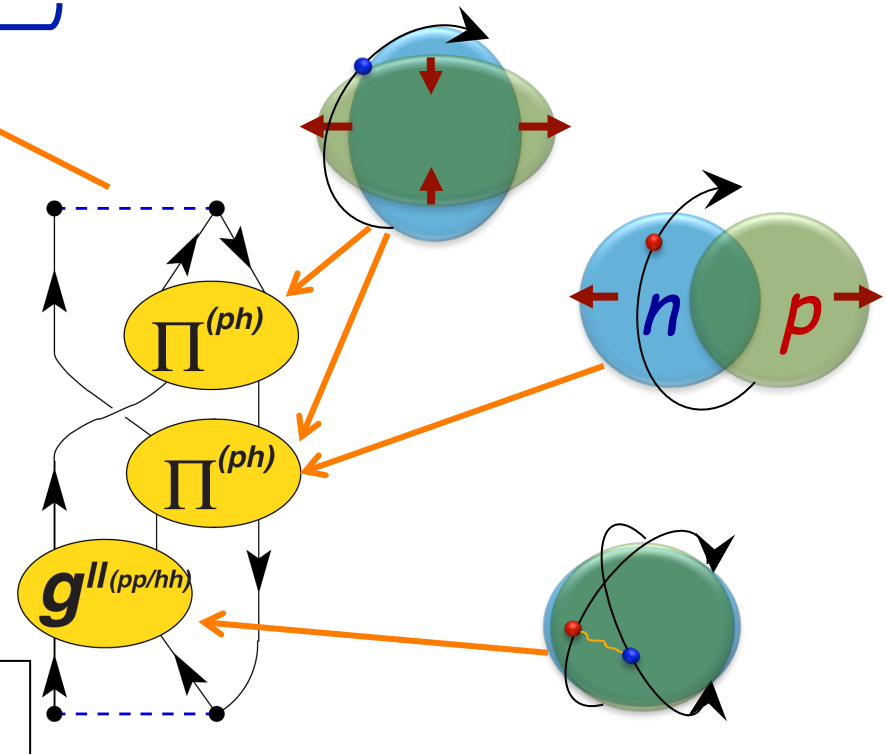
CB et al.,
Phys. Rev. C63, 034313 (2001)
Phys. Rev. A76, 052503 (2007)
Phys. Rev. C79, 064313 (2009)



• A complete expansion requires all types of particle-vibration coupling

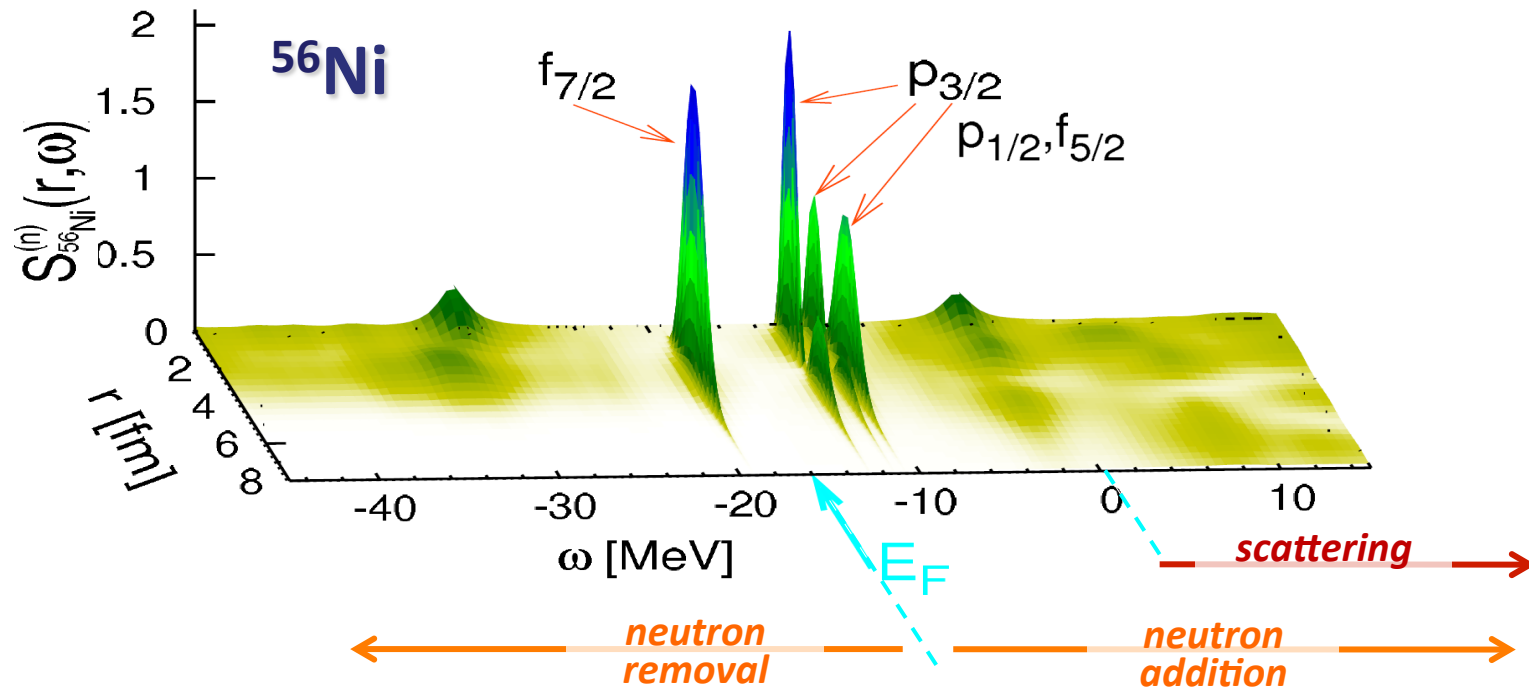
...these modes are all resummed exactly and to all orders in a *ab-initio* many-body expansion.

• The Self-energy $\Sigma^*(\omega)$ yields *both* single-particle states and scattering



One-nucleon spectral function

$$S^{p,h}(r, \omega) = \mp \frac{1}{\pi} \text{Im } g(r = r'; \omega)$$

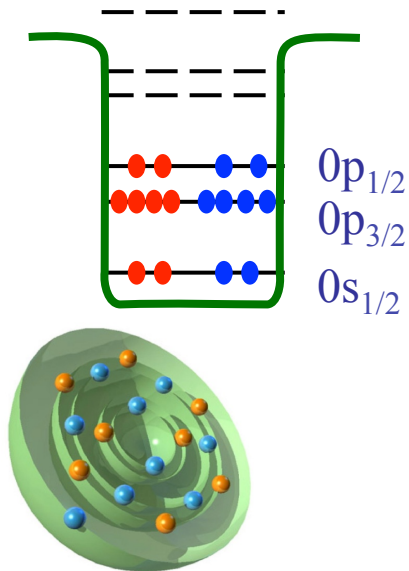


Distribution of particle and hole neutron states in ^{56}Ni

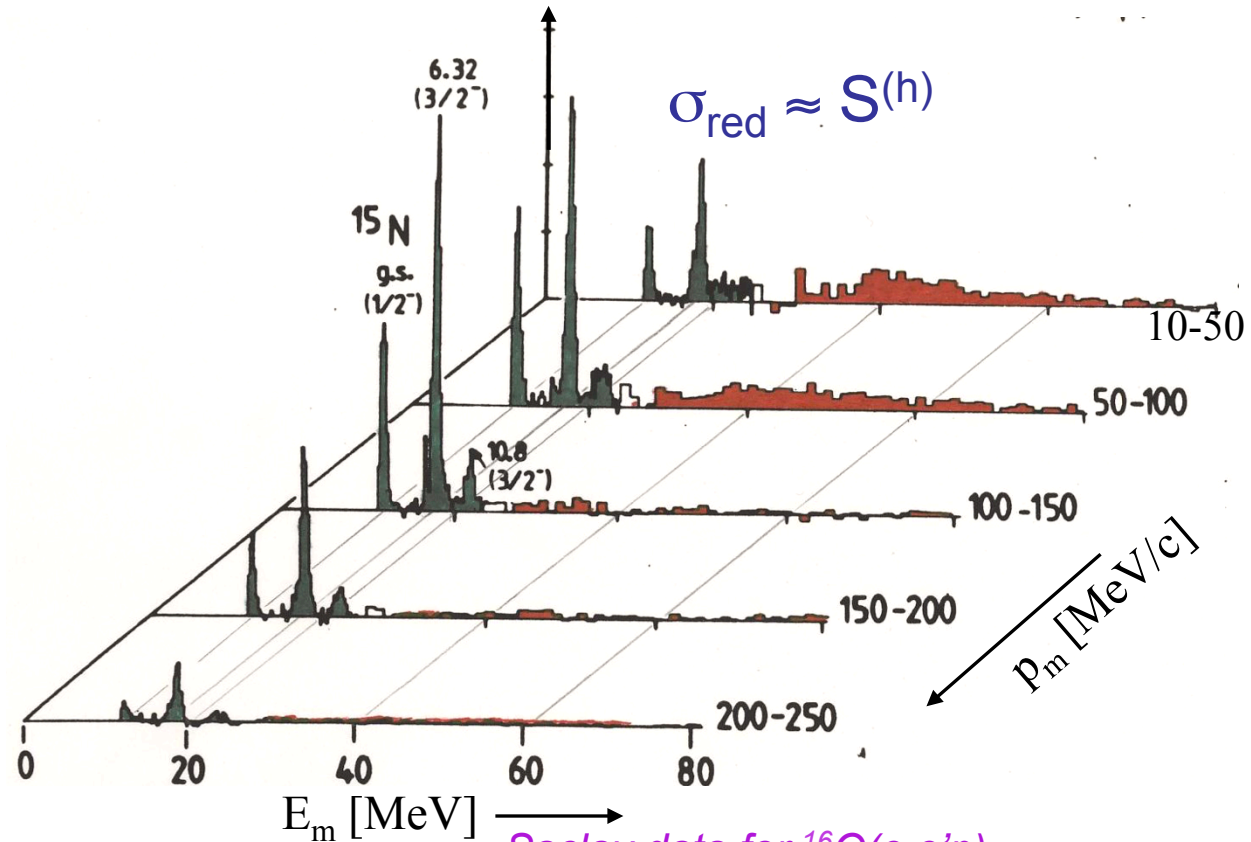
W. Dickhoff, CB, Prog. Part. Nucl. Phys. 53, 377 (2004)
CB, M.Hjorth-Jensen, Pys. Rev. C**79**, 064313 (2009)

Concept of correlations

independent
particle picture



Spectral function: distribution of
momentum (p_m) and energies (E_m)



Saclay data for $^{16}\text{O}(e,e'p)$

[Mougey et al., Nucl. Phys. A335, 35 (1980)]

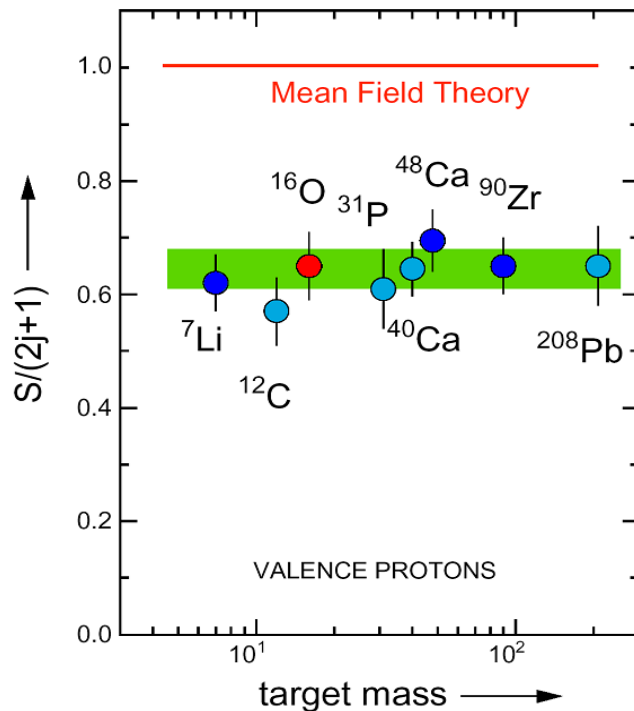
Understood for a few stable closed shells:

[CB and W. H. Dickhoff, Prog. Part. Nucl. Phys 52, 377 (2004)]

Quenching of SF in stable nuclei

Nucl. Phys. A553 (1993) 297c

NIKHEF:



A common *misconception* about SRC :

"The quenching is constant over all stable nuclei, so it must be a short-range effect"



*Actually, **NO!***

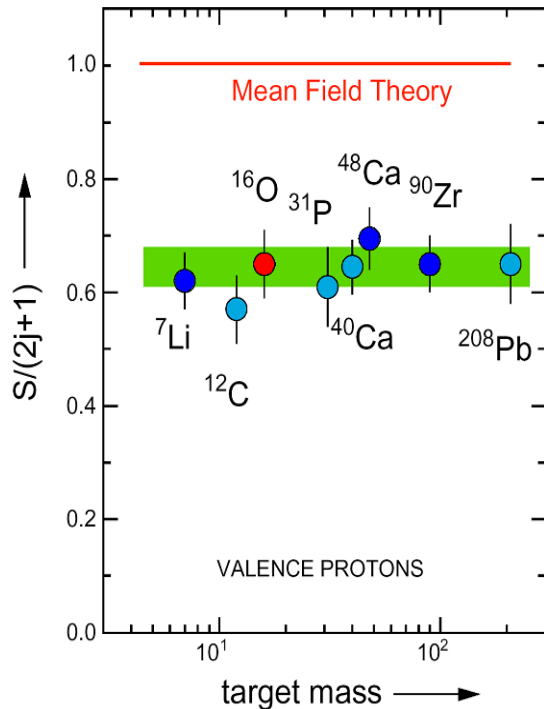
All calculations show that SRC have just a small effect at the Fermi surface. And the correlation to the experimental p-h gap is much more important.

[W. Dickhoff, CB, Prog. Part. Nucl. Phys. **52**, 377 (2004)]

Quenching of SF in stable nuclei

NIKHEF:

Nucl. Phys. A553 (1993) 297c



- Short-range correlations oriented methods:

- VMC [Argonne, '94]
- GF(SRC) [St.Louis-Tübingen '95]
- FHNC/SOC [Pisa '00]

- Including particle-phonon couplings:

- GF(FRPA) [St.Louis '01]
- [CB et al., Phys. Rev. C **65**, (02)]

- Experiment:

$S_{p1/2}$

$S_{p3/2}$

0.90

0.91

0.90

0.89

0.77

0.72

0.63

0.67 ± 0.07
(estimated uncertainty)

SRC are present and verified experimentally

BUT they are NOT the dominant mechanism for quenching SF!!!

Treating short-range corr. with a G -matrix

- The short-range core can be treated by summing ladders outside the model space:

$$\Sigma_{\alpha\beta}^{\text{MF}}(\omega) = i \sum_{\gamma\delta} \int \frac{d\omega'}{2\pi} G_{\alpha\gamma, \delta\beta}(\omega + \omega') g_{\delta\gamma}(\omega') = \text{diagram}$$

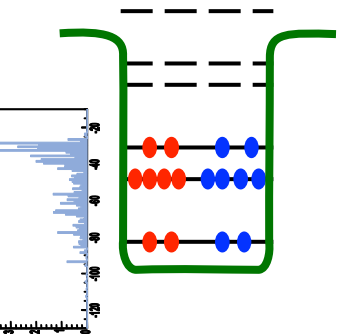
The diagram shows a red wavy line labeled $G(\omega)$ connecting two black dots. The right dot is part of a self-energy loop (a circle with an arrow).

$$\Sigma^*(\mathbf{r}, \mathbf{r}'; \omega) = \Sigma^{\text{MF}}(\mathbf{r}, \mathbf{r}'; \omega) + \tilde{\Sigma}(\mathbf{r}, \mathbf{r}'; \omega).$$

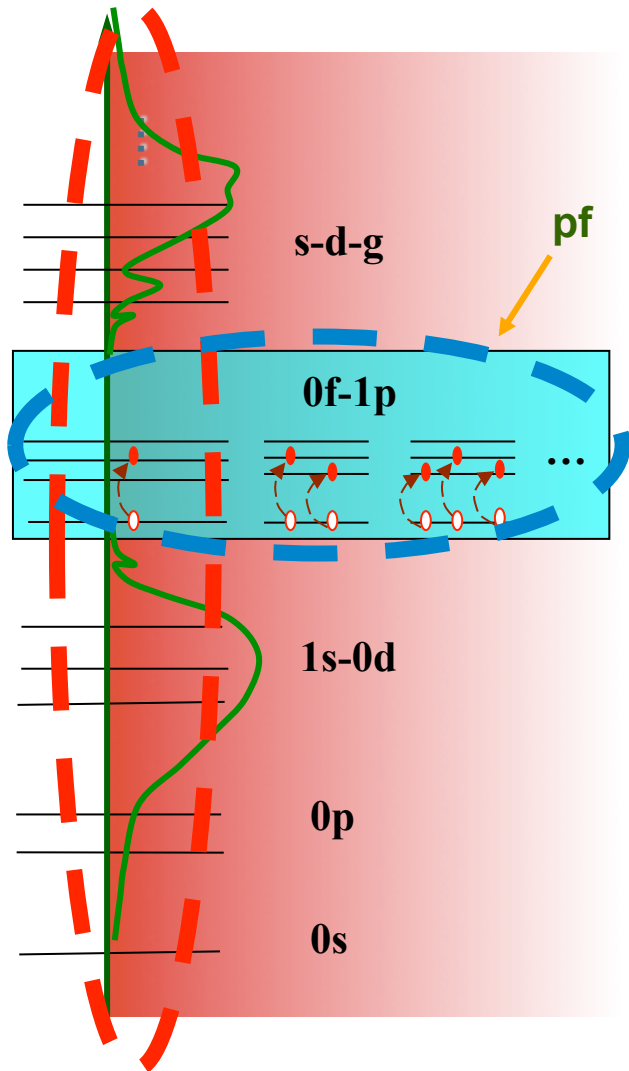
$$Z_\alpha = \int d\mathbf{r} |\psi_\alpha^{A\pm 1}(\mathbf{r})|^2 = \frac{1}{1 - \left. \frac{\partial \Sigma_{\hat{a}\hat{a}}^*(\omega)}{\partial \omega} \right|_{\omega = \pm(E_\alpha^{A\pm 1} - E_0^A)}}$$

Two contributions to the derivative:

- $\Sigma_{\alpha\beta}^{\text{MF}}(\omega)$ is due to scattering to (high-k) states in the Q space
- $\Sigma(\mathbf{r}, \mathbf{r}'; \omega)$ accounts for low-energy (long range) correlations



Quenching of absolute spectroscopic factors



Particle-vibration coupling *dominates* the quenching of spectroscopic factors

Relative strength among fragments *requires* shell-model approach

Quenching of absolute spectroscopic factors

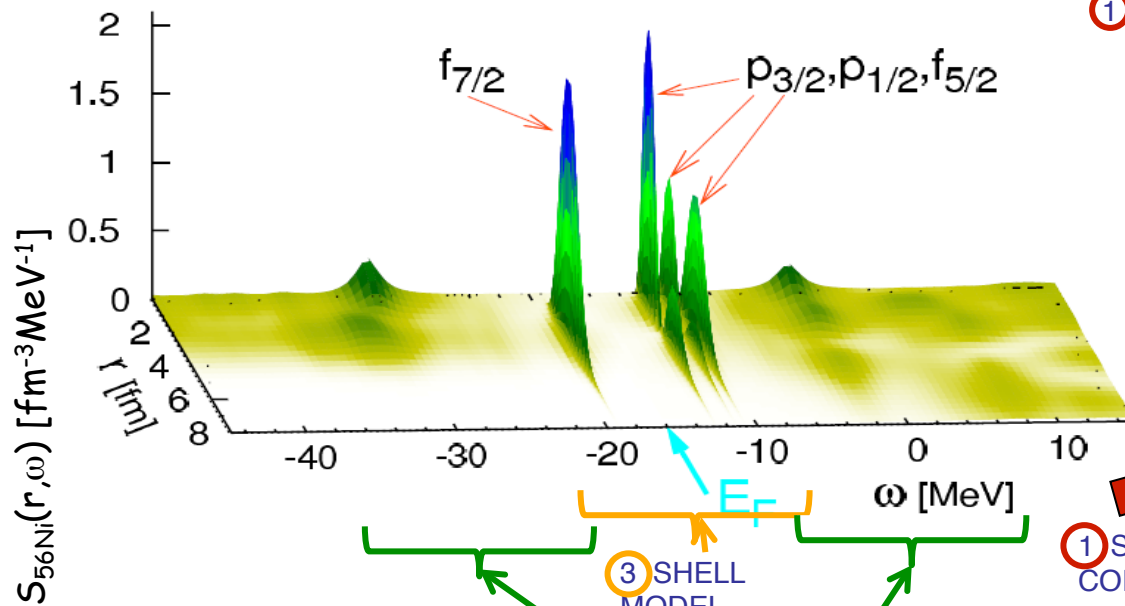
Overall quenching of *spectroscopic factors* is driven by:

SRC → ~10%
part-vibr. coupling → dominant
"shell-model" → in open shell

[CB, Phys. Rev. Lett. **103**, 202520 (2009)]

...with analogous conclusions for ^{48}Ca

	10 osc. shells			Exp. [30]	1p0f space		
	FRPA (SRC)	full FRPA	FRPA + ΔZ_α		FRPA	SM	ΔZ_α
^{57}Ni :							
$\nu 1p_{1/2}$	0.96	0.63	0.61		0.79	0.77	-0.02
$\nu 0f_{5/2}$	0.95	0.59	0.55		0.79	0.75	-0.04
$\nu 1p_{3/2}$	0.95	0.65	0.62	0.58(11)	0.82	0.79	-0.03
^{55}Ni :							
$\nu 0f_{7/2}$	0.95	0.72	0.69		0.89	0.86	-0.03
	①	② + ③			③		



$$Z_\alpha = \int d^3r |\psi_\alpha^{overlap}(\mathbf{r})|^2 = \frac{1}{1 - \left. \frac{\partial \Sigma_{\hat{\alpha}\hat{\alpha}}(\omega)}{\partial \omega} \right|_{\omega=\epsilon_\alpha}}$$

① SHORT RANGE CORRELATIONS

② PARTICLE-VIBRATION COUPLING

③ SHELL MODEL

Dependence of Spect. Fact. from p-h gap

N3LO needs a monopole correction to fix the p-h gap:

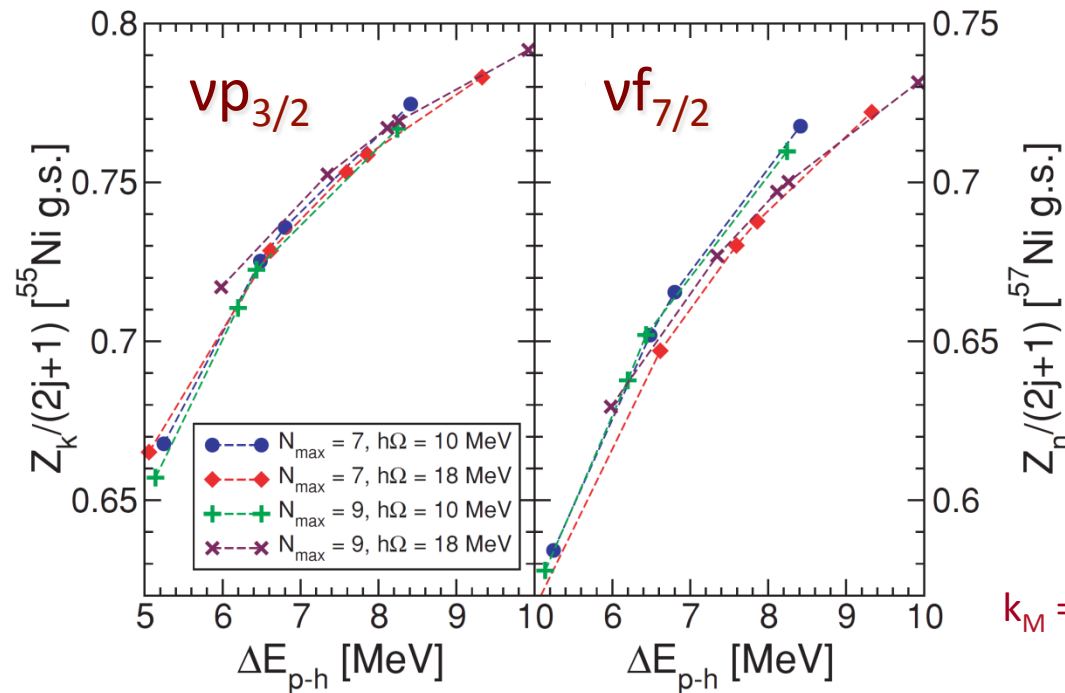
$$\left\{ \begin{array}{l} \Delta V_{fr}^T \rightarrow \Delta V_{fr}^T - (-1)^T \kappa_M, \\ \Delta V_{ff}^T \rightarrow \Delta V_{ff}^T - 1.5(1 - T) \kappa_M, \end{array} \right.$$

$$r \equiv p_{3/2}, p_{1/2}, f_{5/2}$$

$$f \equiv f_{7/2}$$

Experimental Eph

is found for $\kappa_M = 0.57$



$\kappa_M = 0.4-0.7$ MeV

small $\kappa_M \leftarrow$

\rightarrow large κ_M

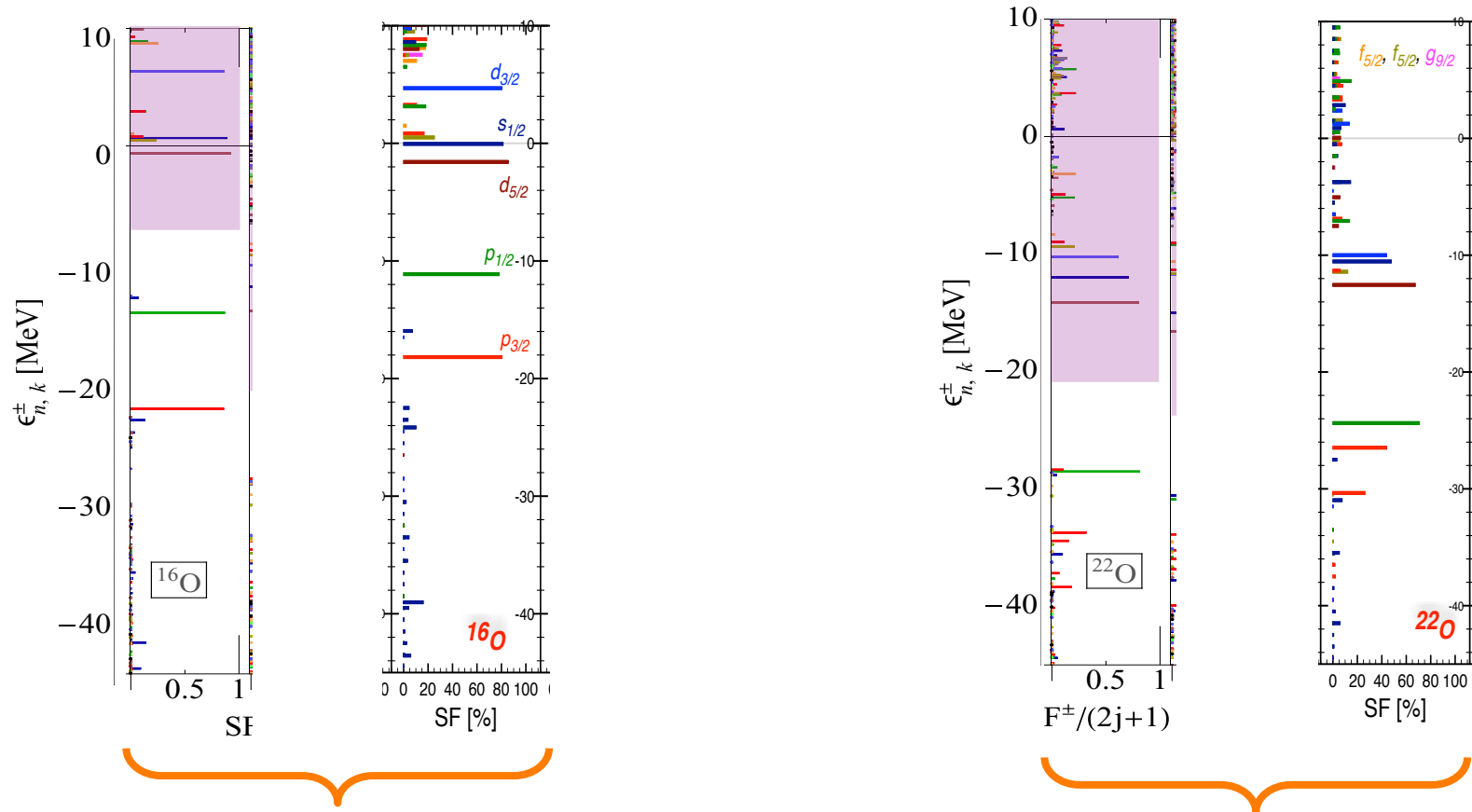
N3LO interaction + monopole corr.

[CB, M.Hjorth-Jensen, Pys.Rev.C79, 064313 (2009)]

Proton spectral strength in Oxygen

A. Cipollone, CB, P. Navrátil, Phys. Rev. Lett. **111**, 062501 (2013)
and Phys. Rev. C **92**, 014306 (2015)
and *in preparation*

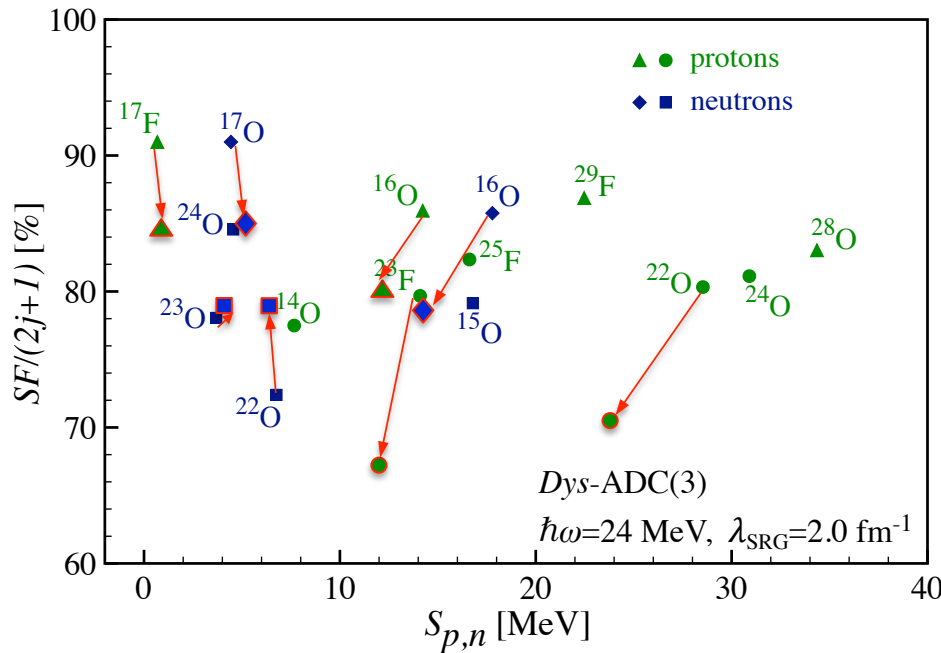
More in detail:



Z/N asymmetry dependence of SFs - Theory

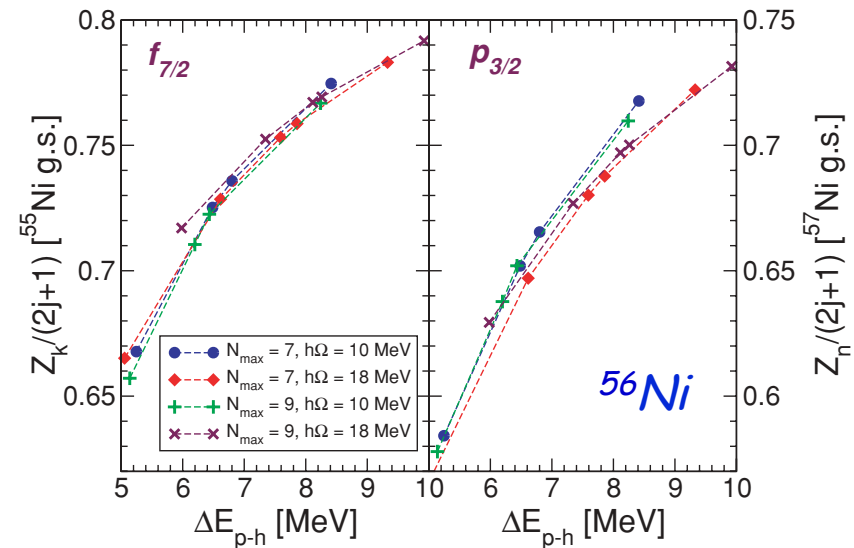
Ab-initio calculations explain (a very weak) the Z/N dependence but the effect is much lower than suggested by direct knockout

Rather the quenching is high correlated to the gap at the Femi surface.



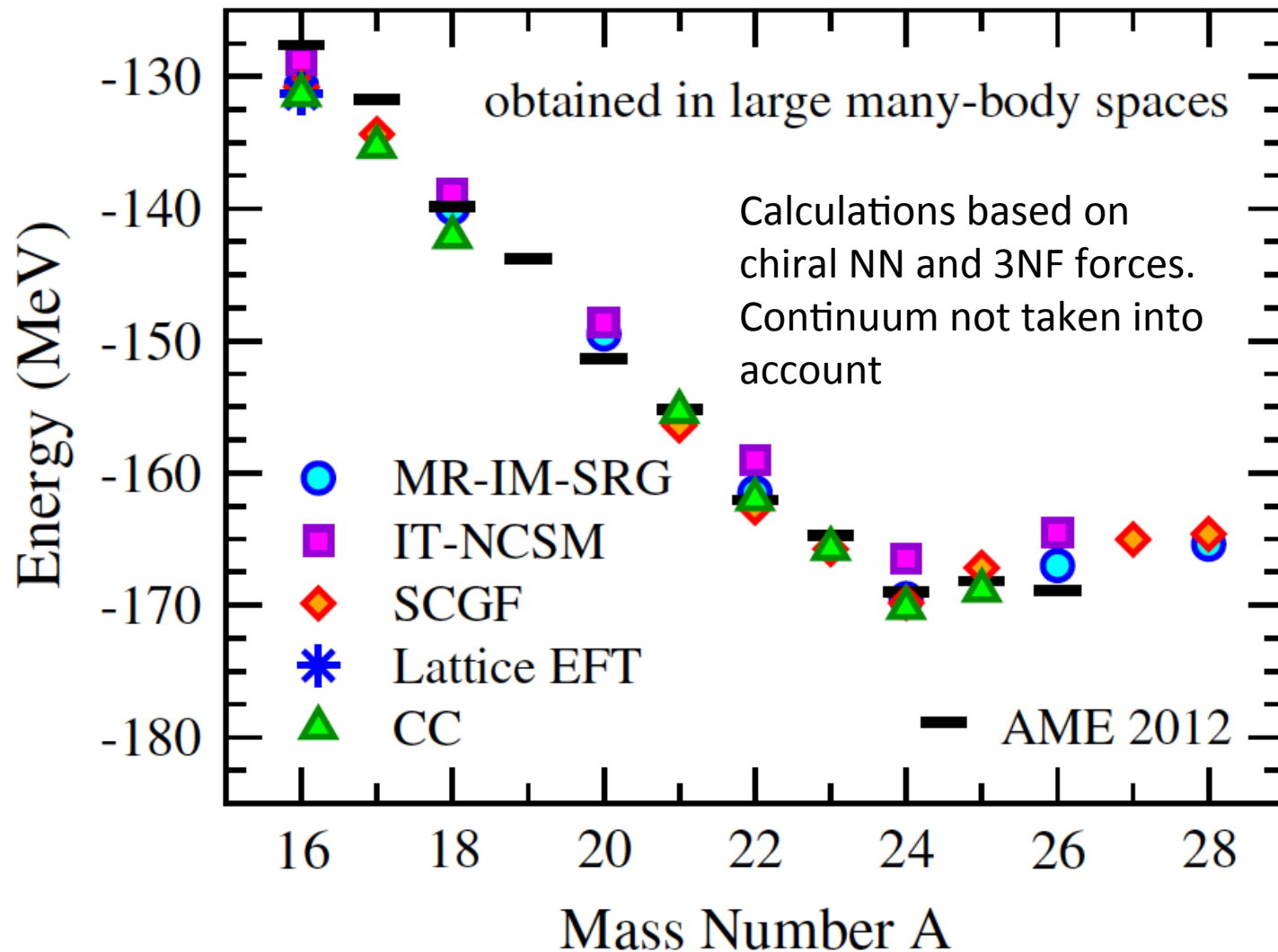
A. Cipollone, CB, P Navrátil
Phys. Rev. C **92**, 014306 (2015)

Spectroscopic factor are strongly correlated to p-h gaps:



CB, M. Hjorth-Jensen,
Phys. Rev. C **79**, 064313 (2009)

Benchmark of *ab-initio* methods in the oxygen isotopic chain

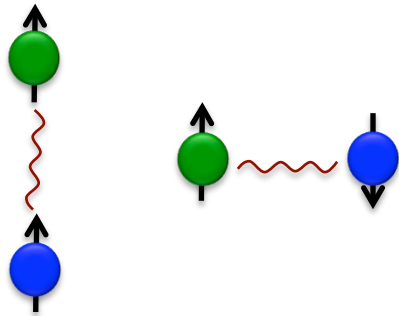


Nuclear forces in exotic nuclei

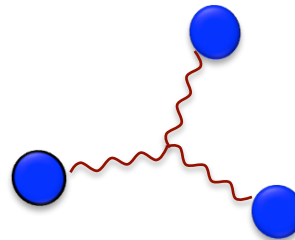
Nucleon interactions are very complex and difficult to handle...

Symmetric matter:
 $N \approx Z$

Tensor force (p-n)



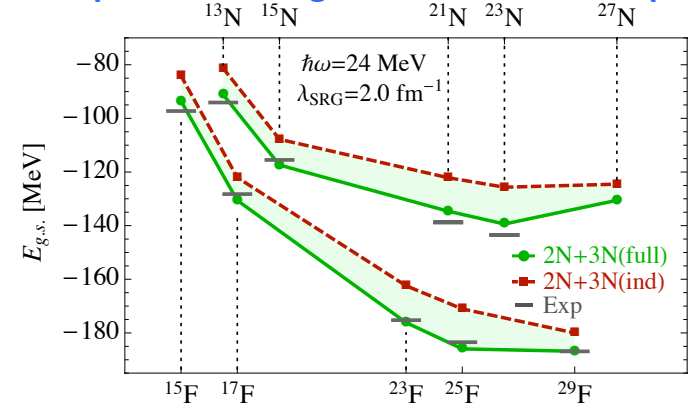
Three-nucleon
Force (3NF)



Neutron-rich matter ($N \gg Z$):

- Neutron star matter EoS
- Symmetry energy
- new shell closures

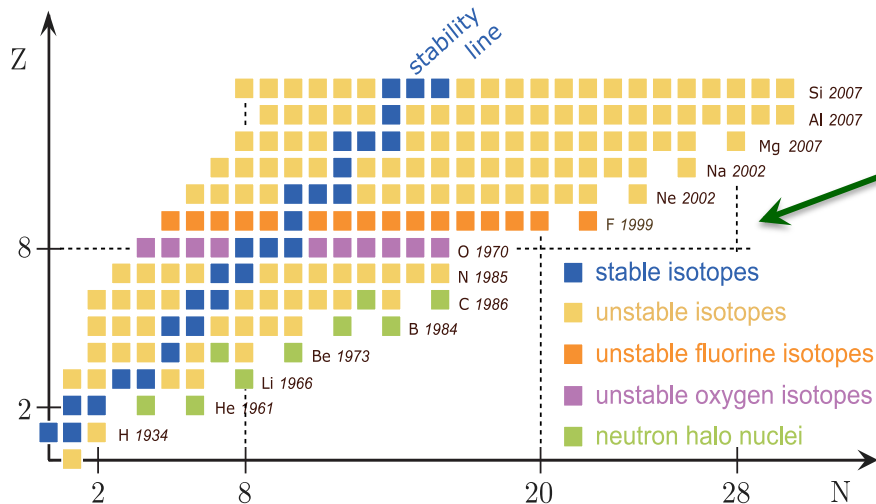
Driplines of nitrogen and fluorine isotopes



[A. Cipollone, CB, P. Navrátil, Phys. Rev. Lett. **111**, 062501 (2013)]

Change of regime from
stable to dripline isotopes !

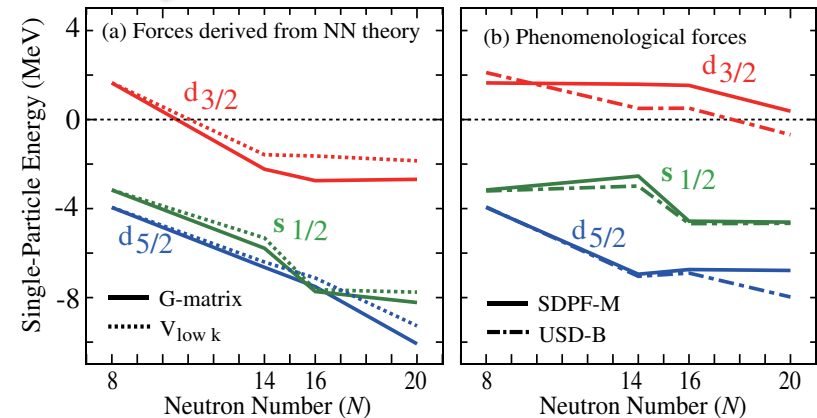
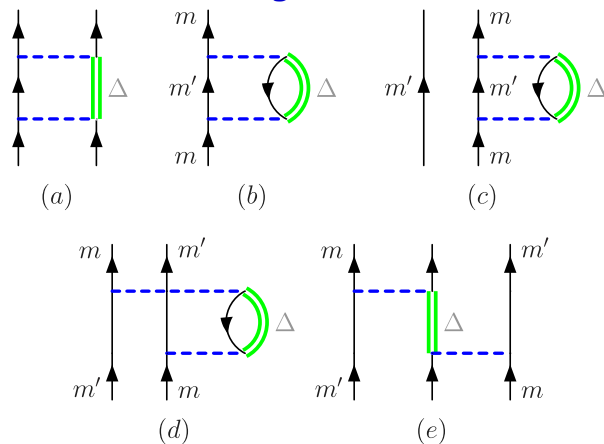
Oxygen puzzle...



The oxygen dripline is at ^{24}O , at odds with other neighbor isotope chains.

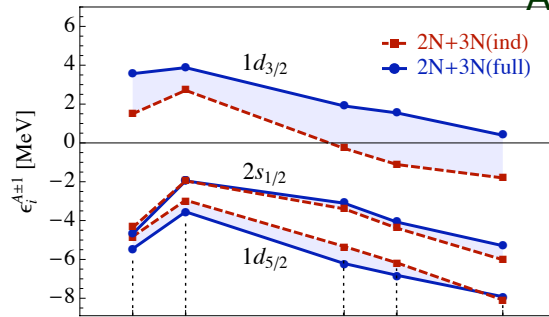
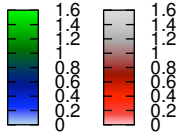
Phenomenological shell model interaction reflect this in the s.p. energies but no realistic NN interaction alone is capable of reproducing this...

The fujita-Miyazawa 3NF provides repulsion through Pauli screening of other 2NF terms:

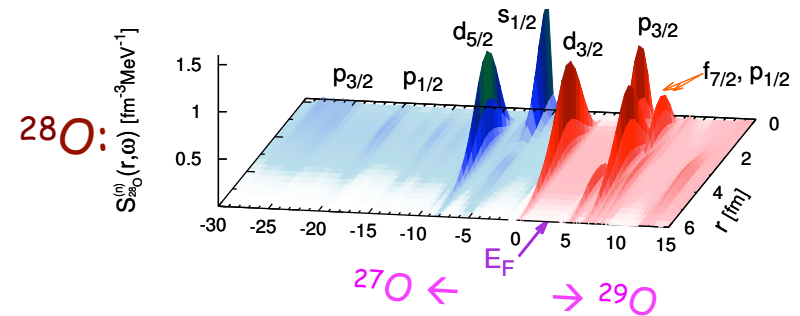
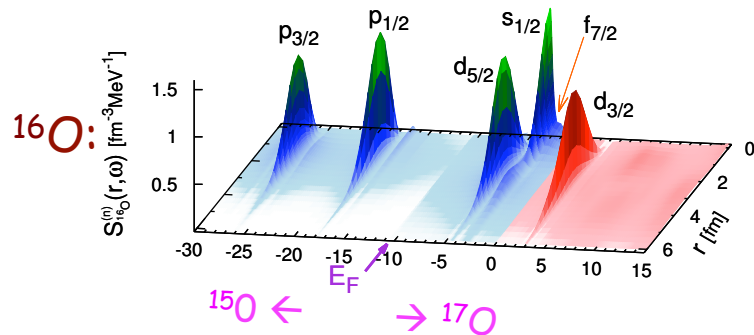
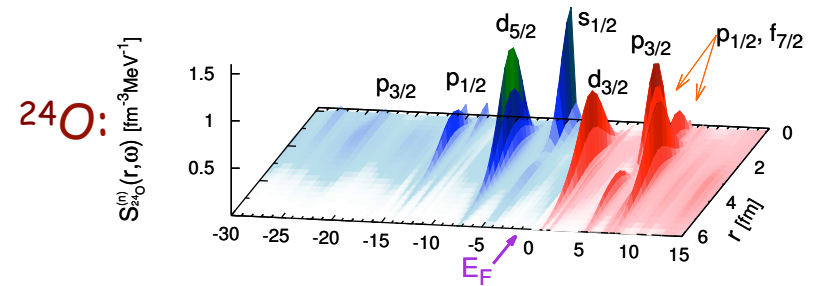
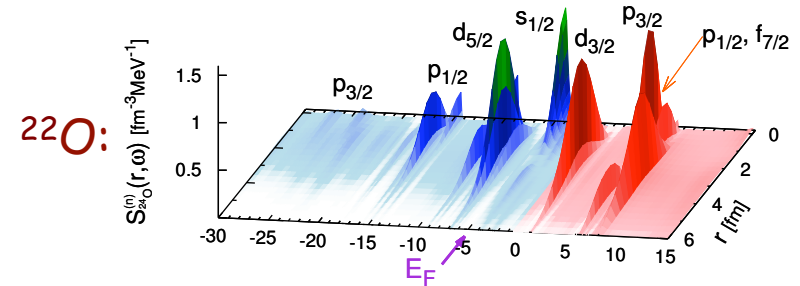
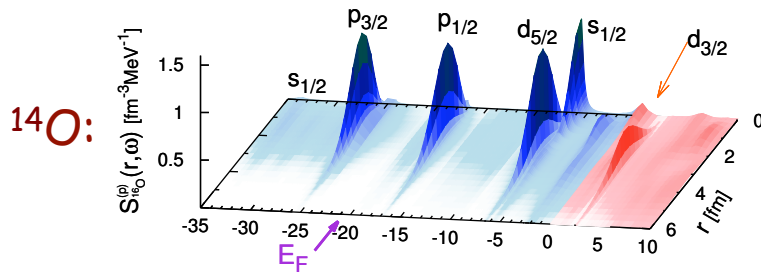


[T. Otsuka et al., Phys Rev. Lett **105**, 32501 (2010)]

Neutron spectral function of Oxygens

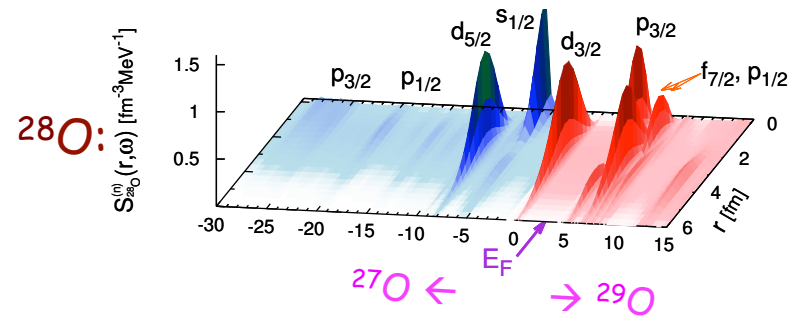
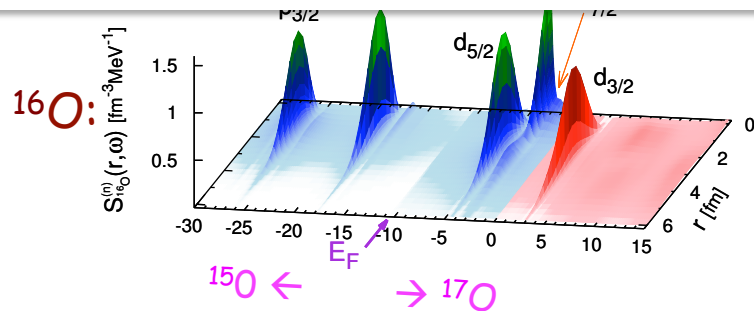
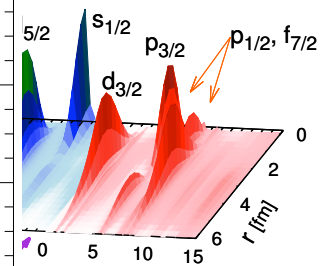
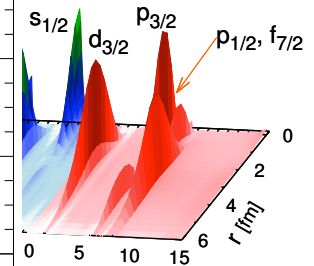
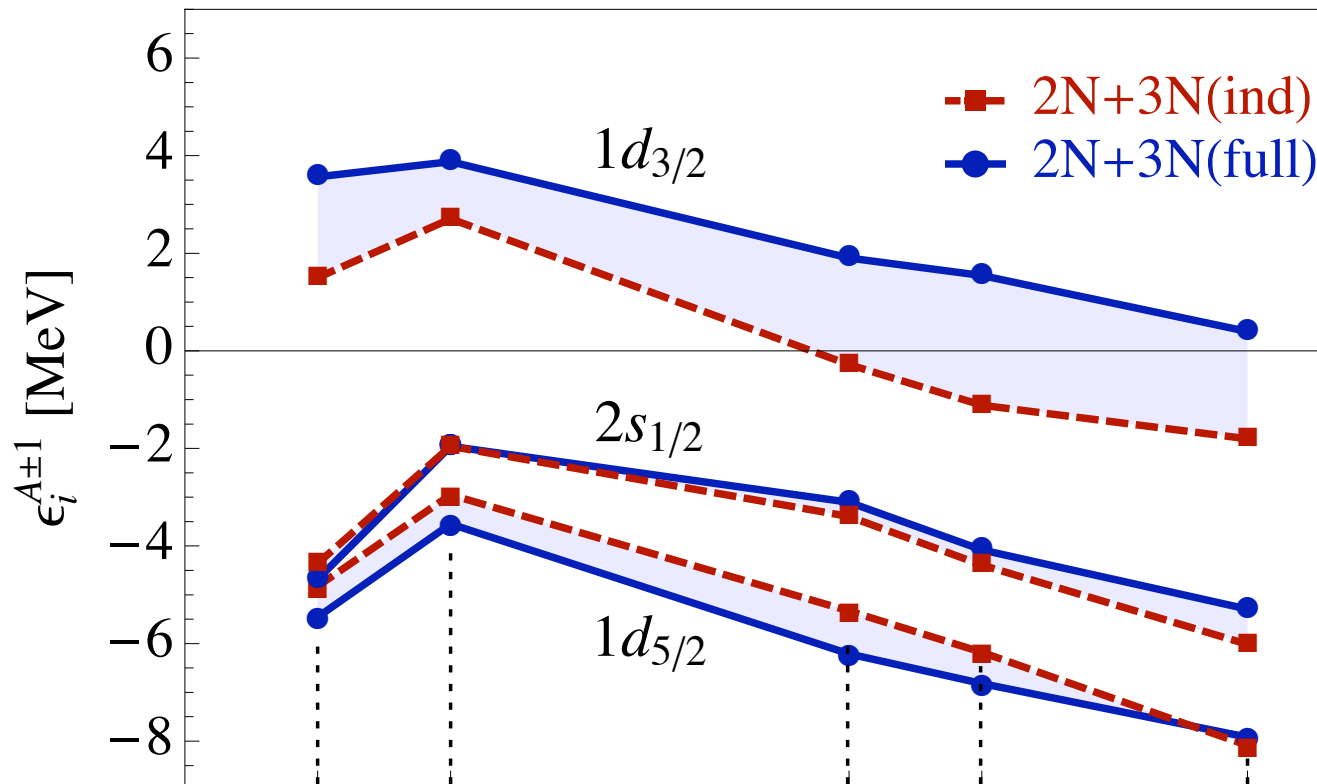


A. Cipollone, CB, P. Navrátil, *Phys. Rev. C* **92**, 014306 (2015)



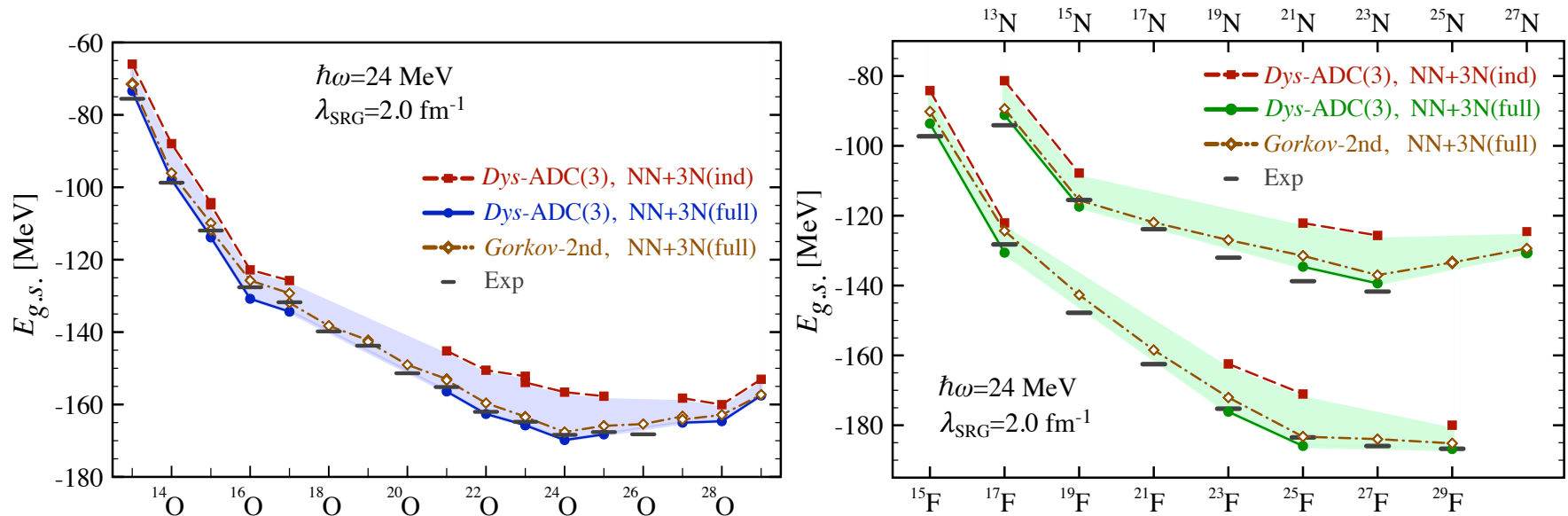
Neutron spectral function of Oxygens

Rev. C 92, 014306 (2015)



Results for the N-O-F chains

A. Cipollone, CB, P. Navrátil, Phys. Rev. Lett. **111**, 062501 (2013)
and Phys. Rev. C **92**, 014306 (2015)



→ 3NF crucial for reproducing binding energies and driplines around oxygen

→ cf. microscopic shell model [Otsuka et al, PRL**105**, 032501 (2010).]



Radii and Binding Energies in Oxygen Isotopes: A Challenge for Nuclear Forces

V. Lapoux,^{1,*} V. Somà,¹ C. Barbieri,² H. Hergert,³ J. D. Holt,⁴ and S. R. Stroberg⁴

- New fits of chiral interactions (NNLO_{sat}) highly improve comparison to data

- Deficiencies remain for neutron rich isotopes

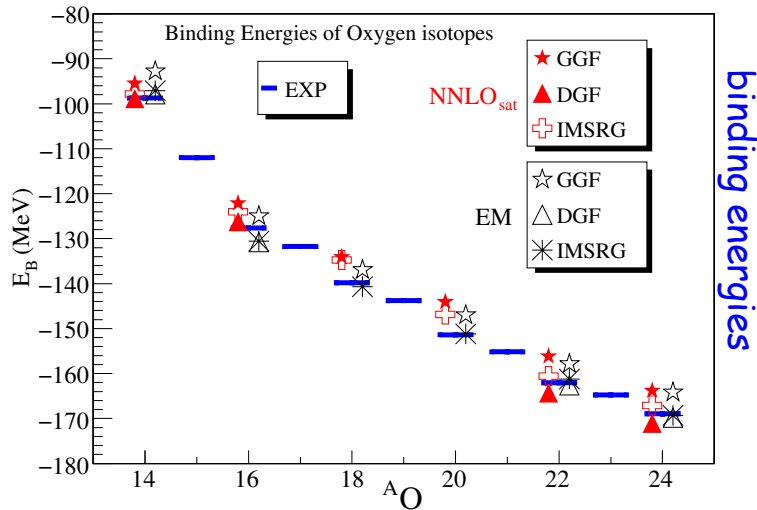
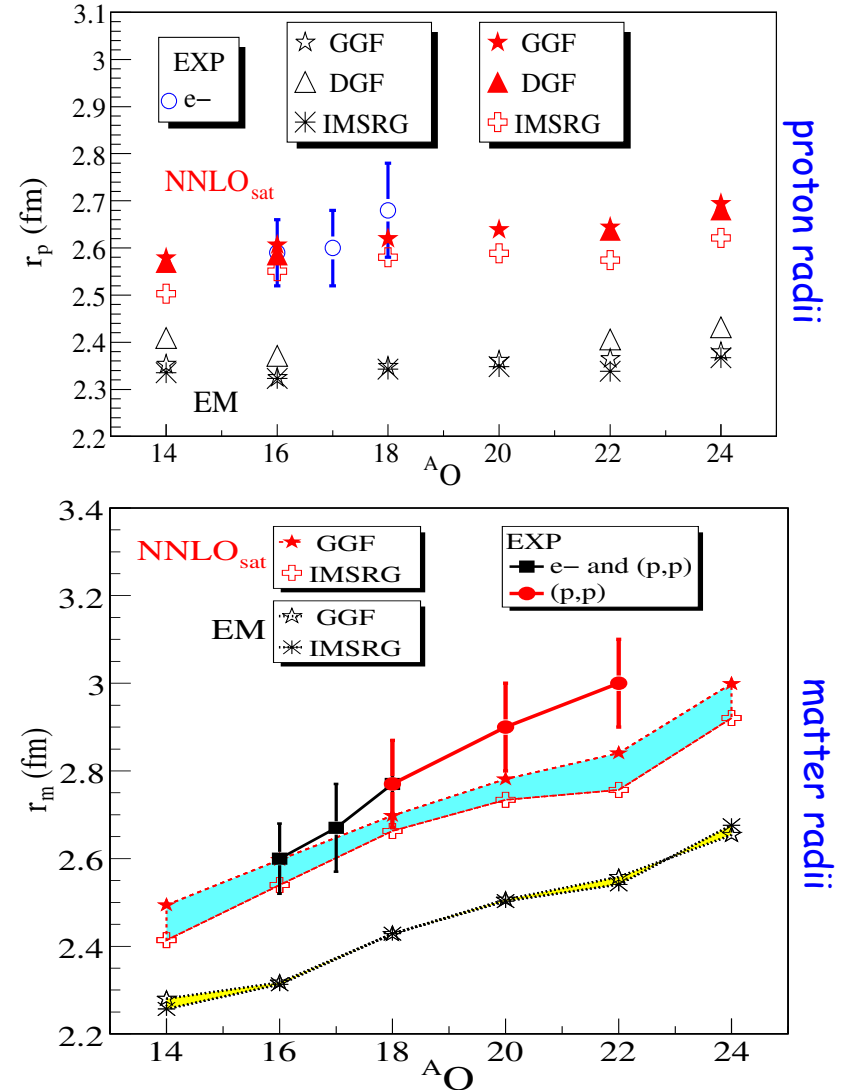


FIG. 1. Oxygen binding energies. Results from SCGF and IMSRG calculations performed with EM [20–22] and NNLO_{sat} [26] interactions are displayed along with available experimental data.

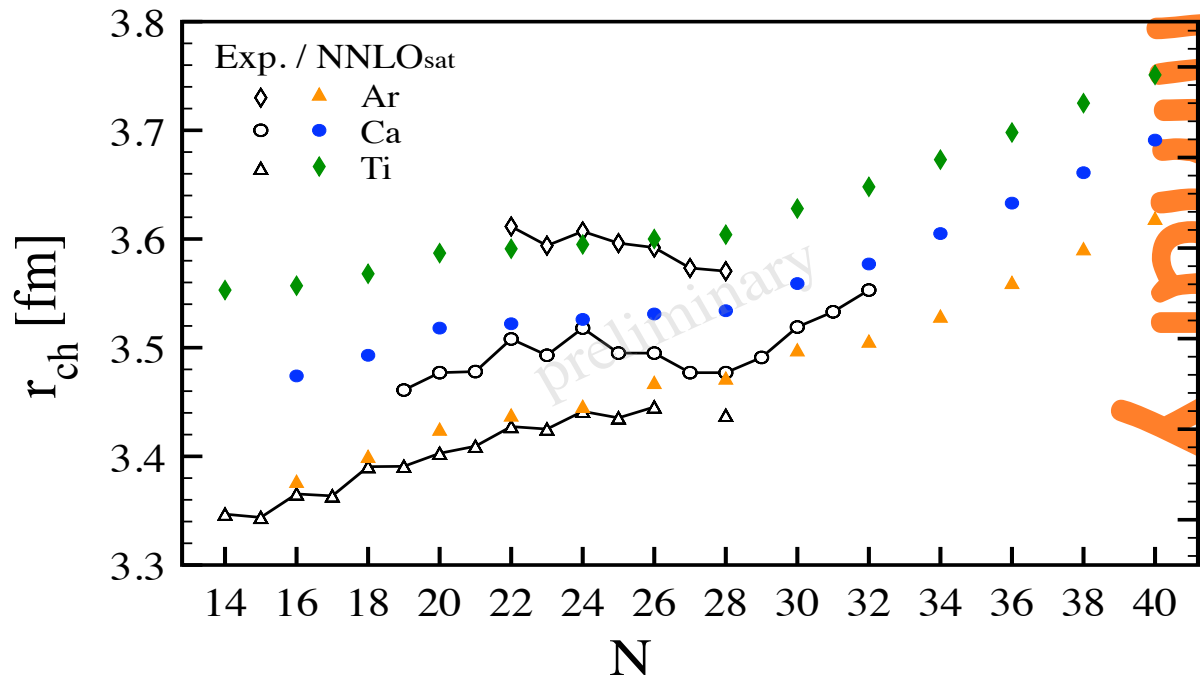
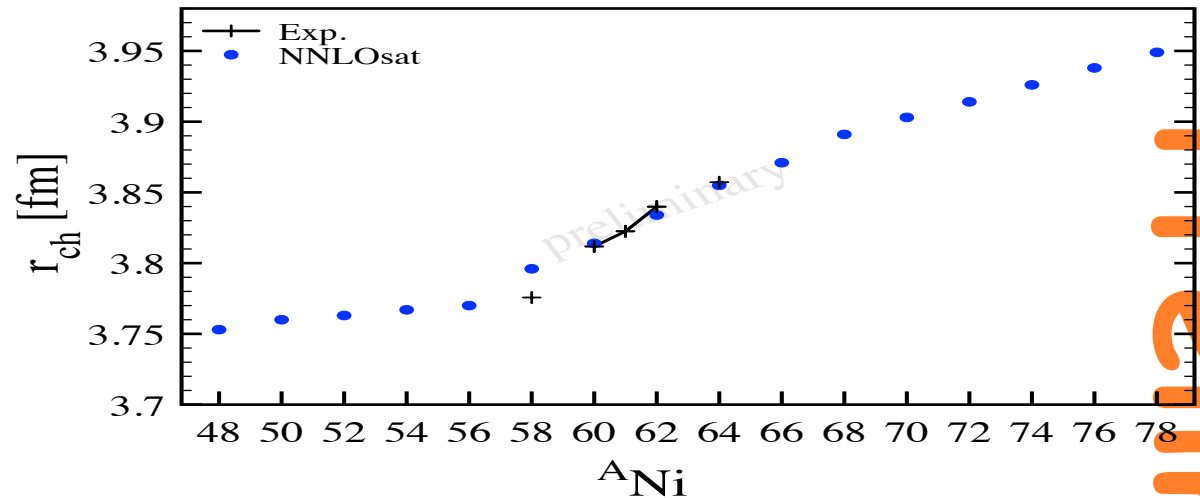


charge radii in the pf shell

Size of radii not perfect but remains overall correct throughout the *pf* shell with NNLO-sat.

This suggests that saturation is indeed under control.

→ Improvements of many-body truncations beyond 2nd order Gorkov will also be relevant.
(work in progress!)

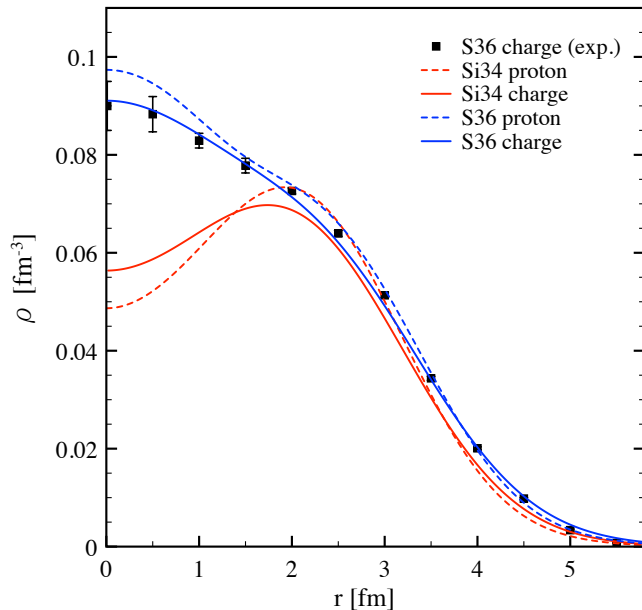


Preliminary

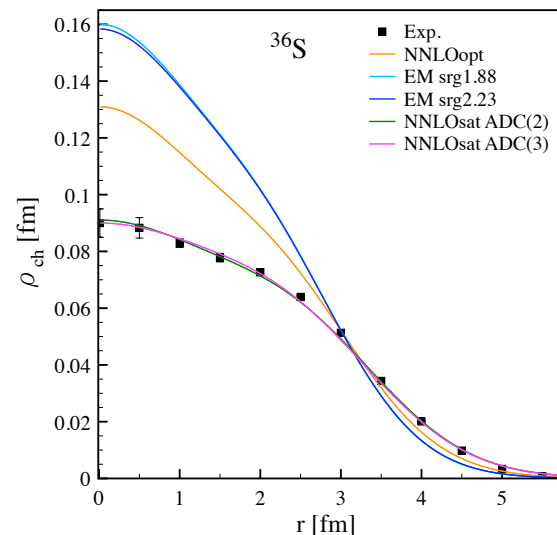
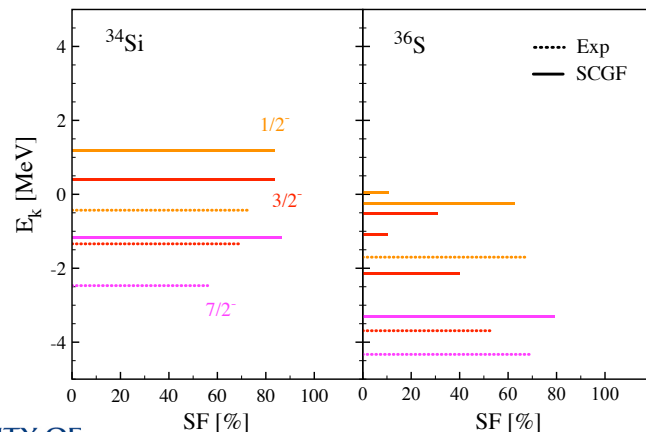
Bubble nuclei... ^{34}Si prediction

Duguet, Somà, CB, et al. arXiv:1611.08570 [nucl-th]

- ^{34}Si is unstable, charge distribution still unknown
- Suggested central depletion from mean-field simulations
- *Ab-initio* theory confirms predictions

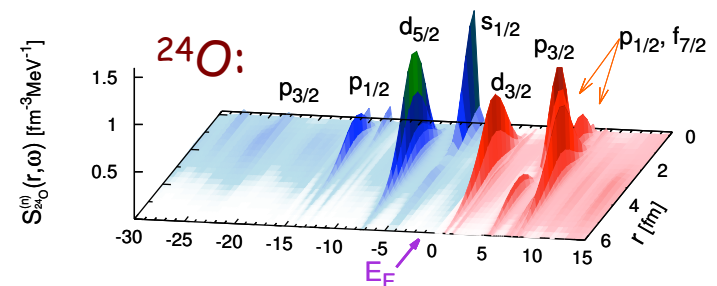


Validated by charge distributions and neutron quasiparticle spectra:



Some considerations:

- Emergence of shell effects is trivially linked to the size of a nuclear well
→ Nuclear radii are the most important constraint
- However:
 - actual "shell structure" is highly linked to details of the nuclear force
 - 3NF and spin-orbit change shell ordering and limit of stability
- Phenomenological understanding of atomic nuclei seem (so far) well explained by underlying theories
- Deeper understanding of macroscopic dynamics better understood from larger scales??



Thank you for your attention!!!

Collaborators



A. Cipollone, C. McIlroy
A. Rios, A. Idini, F. Raimondi



A. Polls



energie atomique • energies alternatives

V. Somà, T. Duguet



**W.H. Dickhoff,
S. Waldecker**



A. Carbone



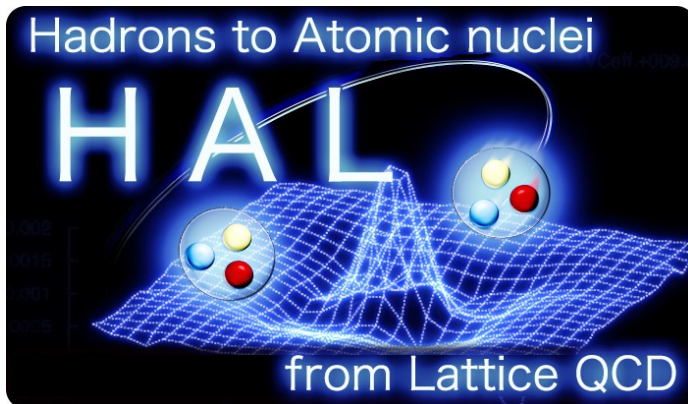
D. Van Neck,



P. Navratil



M. Hjorth-Jensen



S. Aoki,
T. Doi, T. Hatsuda, Y. Ikeda,
T. Inoue,
N. Ishii, K. Murano,
H. Nemura, K. Sasaki
F. Etminan
T. Miyamoto,
T. Iritani
S. Gongyo

YITP Kyoto Univ.
RIKEN Nishina
Nihon Univ.
RCNP Osaka Univ
Univ. Tsukuba
Univ. Birjand
Univ. Tsukuba
Stony Brook Univ.
YITP Kyoto Univ.